

Stochastic modeling of the oceanic mesoscale eddies

The 6th STUDO Sandbox Workshop — 12 February 2021

Long Li¹, Bruno Deremble², Noé Lahaye¹ and Etienne Mémin¹

¹ *Inria Rennes Bretagne Atlantique, France*

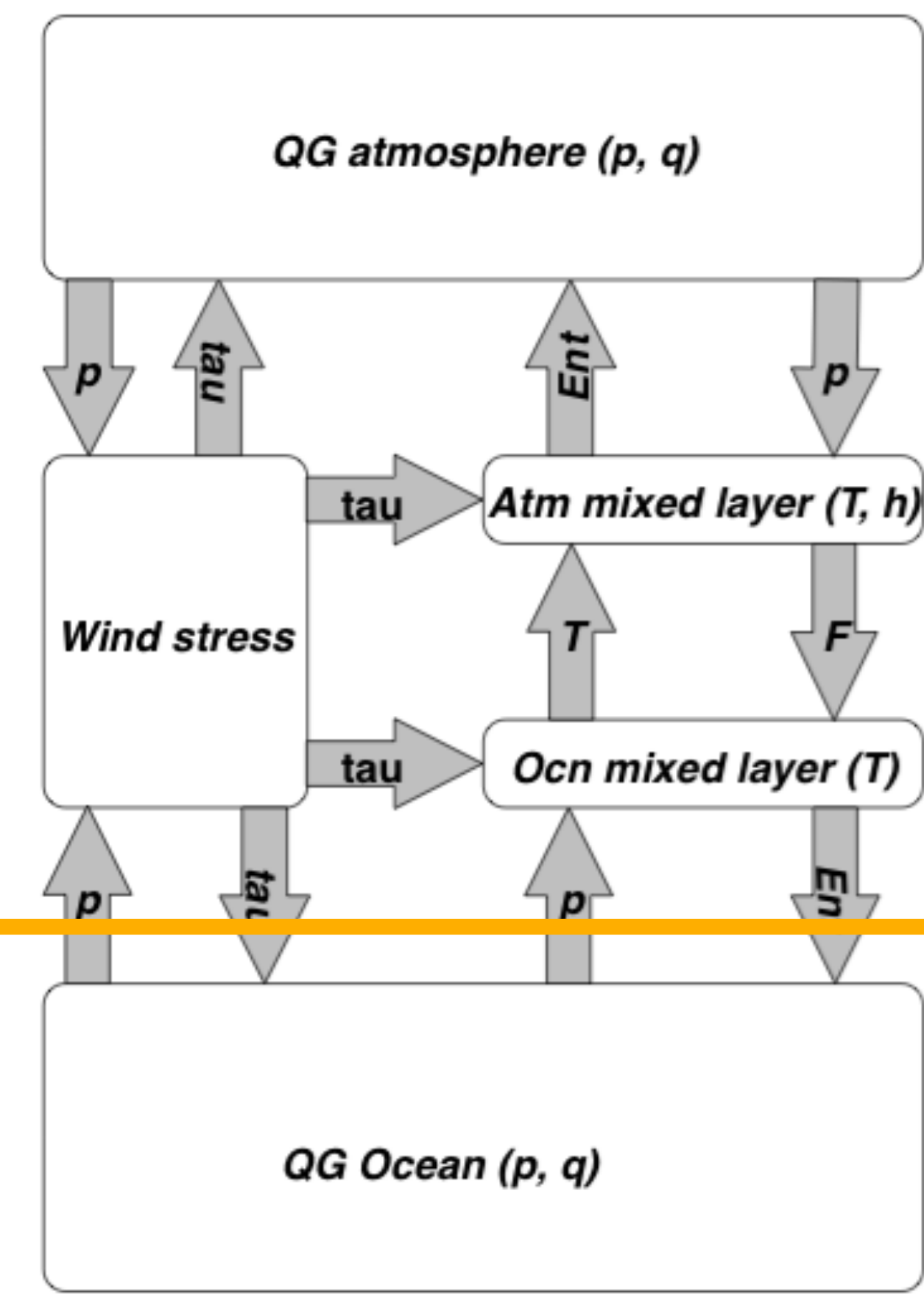
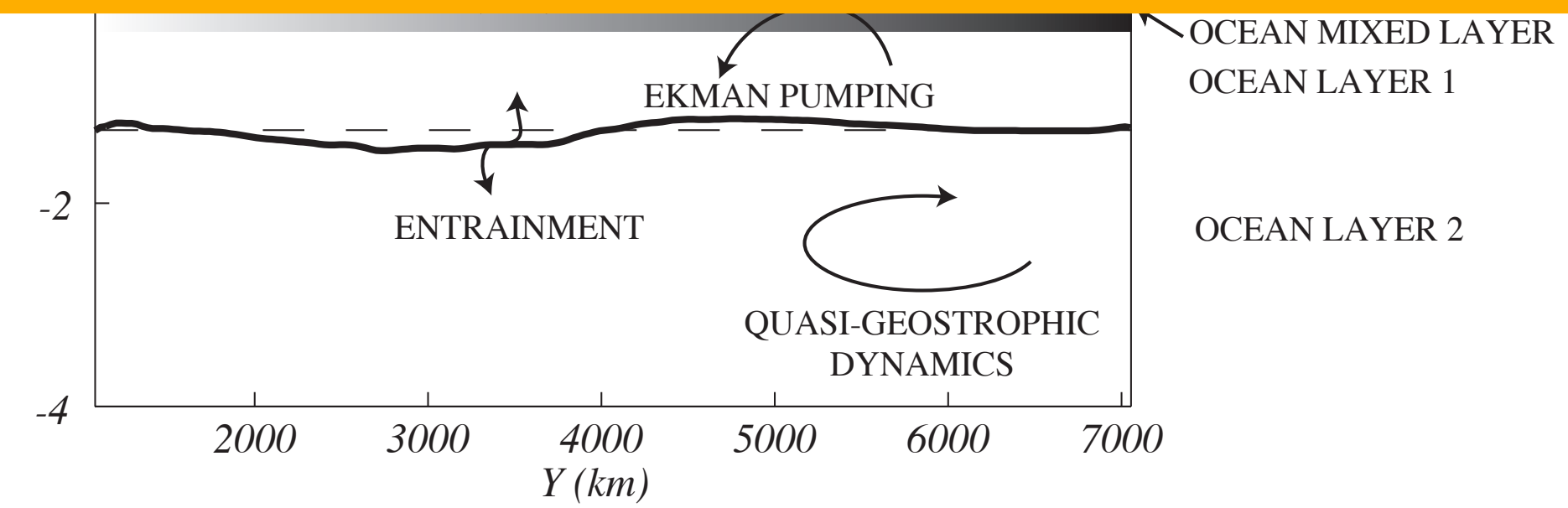
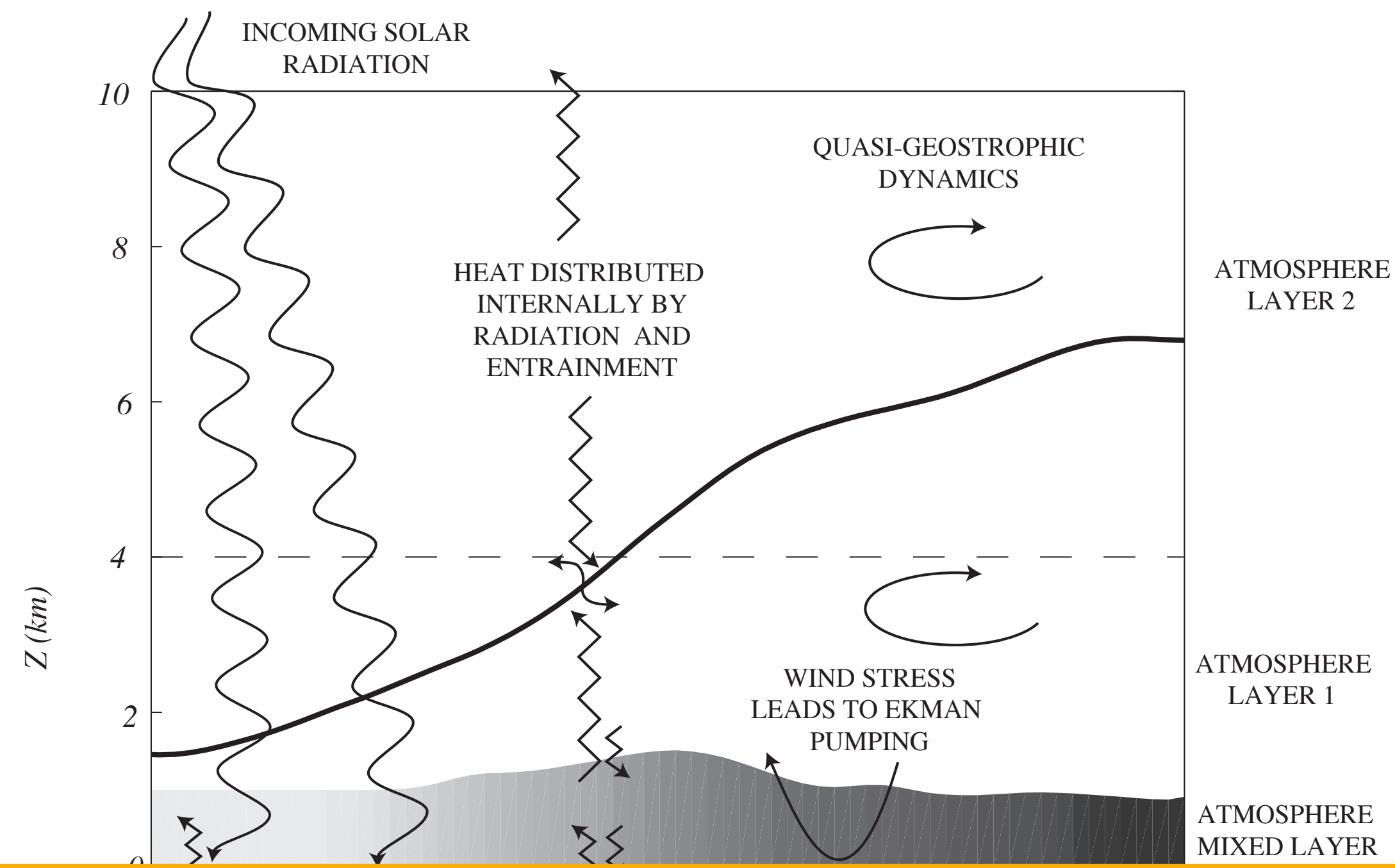
² *Institut des Géosciences de l'Environnement, France*



Motivations

- I. Can LU model better represent the mesoscale eddies effect on the large-scale circulation?
- II. Can LU model improve the internal variability of coarse-resolution ocean models?

Dynamical core



Quasi-Geostrophic Coupled Model (Q-GCM) [<http://q-gcm.org>]

Deterministic QG equations

Exp.2

- Evolution of k -th layer potential vorticity (PV)

$$\partial_t q_k = - \nabla \cdot (\mathbf{u}_k q_k) + \frac{A_2}{f_0} \nabla^4 p_k - \frac{A_4}{f_0} \nabla^6 p_k - \frac{f_0}{H_k} (w_k - w_{k-1})$$

- Update k -th layer pressure, height and velocity

$$q_k = \frac{1}{f_0} \nabla^4 p_k + \beta(y - y_0) + \frac{f_0}{H_k} (\eta_k - \eta_{k-1})$$

$$\eta_k = \frac{p_{k+1} - p_k}{g'_k}, \quad g'_k = \frac{g(\rho_{k+1} - \rho_k)}{\rho_0}$$

$$\mathbf{u}_k = \frac{1}{f_0} \nabla^\perp p_k$$

Exp.1

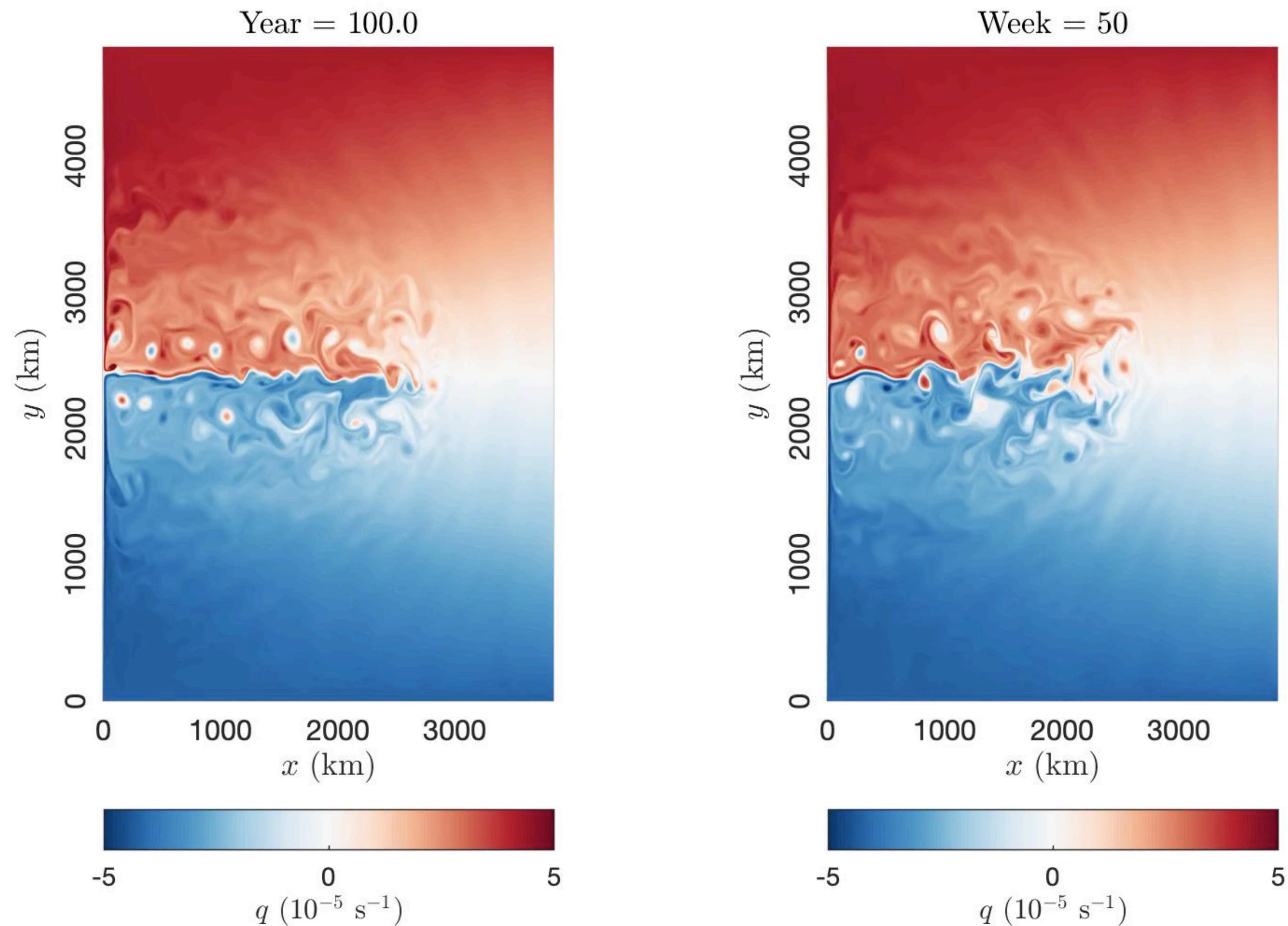
- Evolution of mixed layer temperature (or SST)

$$\mathbf{u}_m = \mathbf{u}_1 + \frac{\boldsymbol{\tau}^\perp}{f_0 H_m}$$

$$\partial_t T_m = - \nabla \cdot (\mathbf{u}_m T_m) + K_2 \nabla^2 T_m - K_4 \nabla^4 T_m + w_0 \frac{T_1 + T_m}{2H_m} - F_m$$

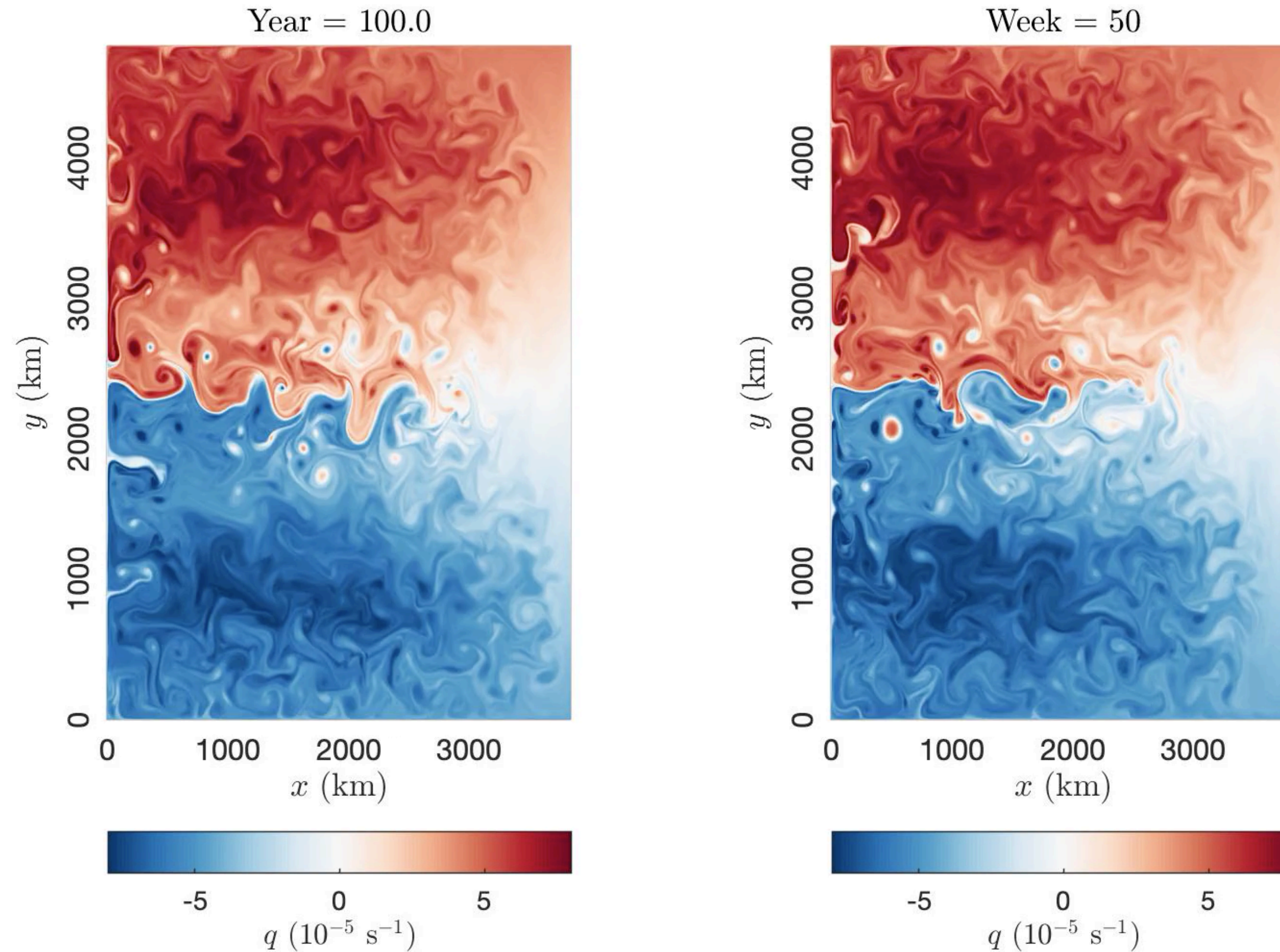
$$w_1 = - \frac{\Delta_m T}{2\Delta_1 T} w_0$$

Eddy-resolving simulations



Upper-layer PV ($\Delta x = 5$ km, $L_d = [39, 22]$ km) of Exp.1 (without SST)

Eddy-resolving simulations



Upper-layer PV ($\Delta x = 5$ km, $L_d = [39, 22]$ km) of Exp.2 (with SST)

Stochastic QG equations

• k -th layer eddy velocity noise (m/s) $\sigma_k \dot{B}_t$

• k -th layer variance tensor (m²/s²) $\frac{a_k}{dt} = \mathbb{E} \left[(\sigma_k \dot{B}_t - \mathbb{E}[\sigma_k \dot{B}_t]) (\sigma_k \dot{B}_t - \mathbb{E}[\sigma_k \dot{B}_t])^T \right]$

• **Evolution of k -th layer PV** $\partial_t q_k = - \nabla \cdot (\mathbf{u}_k q_k) + \frac{A_2}{f_0} \nabla^4 p_k - \frac{A_4}{f_0} \nabla^6 p_k - \frac{f_0}{H_k} (w_k - w_{k-1}) + \nabla \cdot \mathbf{F}_k$

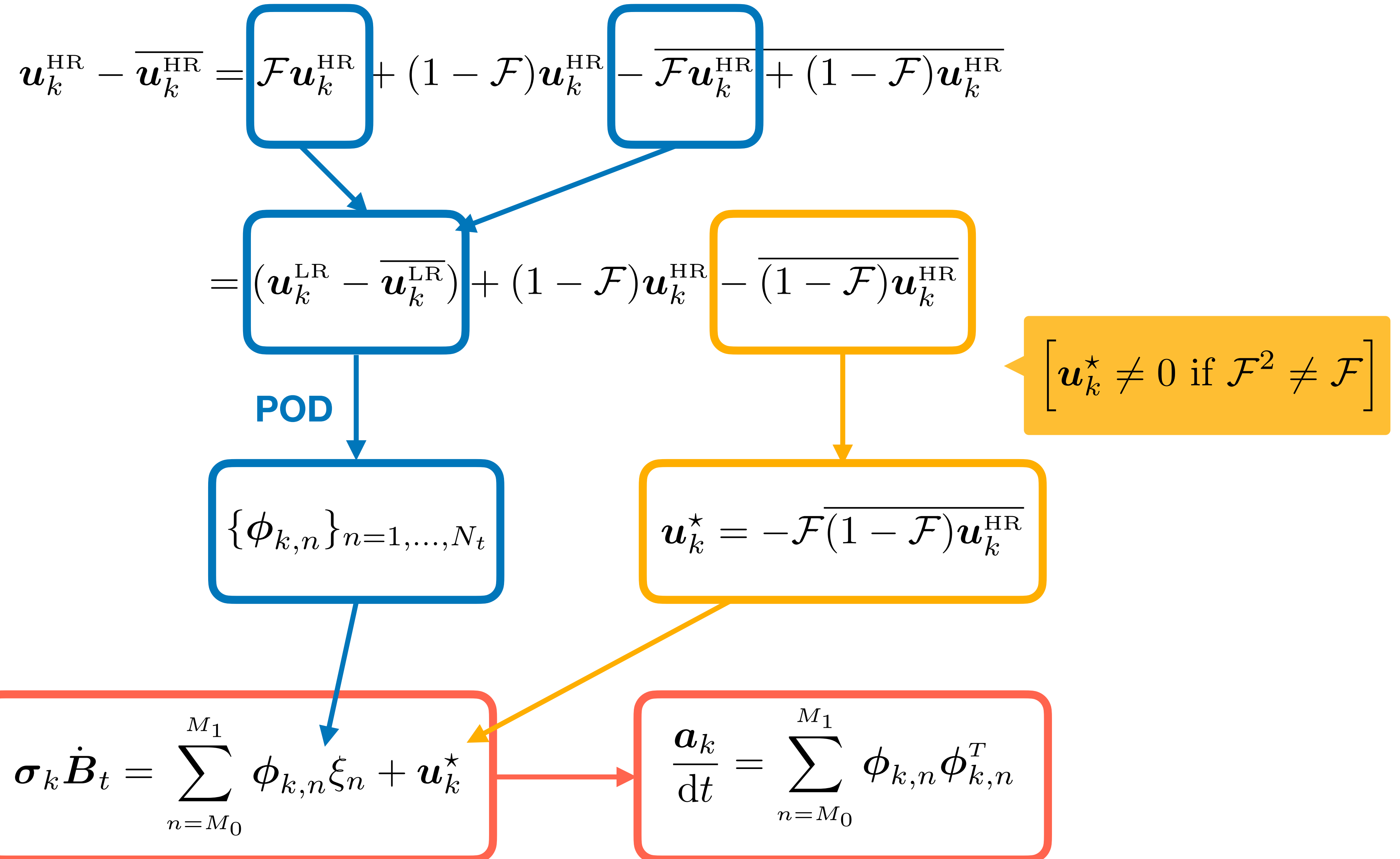
$$\mathbf{F}_k = \underbrace{-\left(\sigma_k \dot{B}_t - \frac{1}{2} \nabla \cdot \mathbf{a}_k\right) q_k}_{\text{Advection flux}} + \underbrace{\frac{1}{2} \mathbf{a}_k \nabla q_k}_{\text{Diffusion flux}} + \underbrace{\left(\mathbf{u}_k \cdot \nabla^\perp \sigma_k \dot{B}_t + \mathbf{a}_k \nabla f\right)}_{\text{Sources flux}} + \underbrace{\frac{1}{2} \sum_{i=1,2} \partial_{x_i}^\perp \mathbf{a}_k \nabla u_k^i}_{\text{Sinks flux}}$$

• **Evolution of SST** $\partial_t T_m = - \nabla \cdot (\mathbf{u}_m T_m) + K_2 \nabla^2 T_m - K_4 \nabla^4 T_m + w_0 \frac{T_1 + T_m}{2H_m} - F_m + \nabla \cdot \mathbf{F}_m$

$$\mathbf{F}_m = \underbrace{-\left(\sigma_1 \dot{B}_t - \frac{1}{2} \nabla \cdot \mathbf{a}_1\right) T_m}_{\text{Advection flux}} + \underbrace{\frac{1}{2} \mathbf{a}_1 \nabla T_m}_{\text{Diffusion flux}}$$

Data-driven modeling

(i) LU-POD



$$\begin{aligned}
 \xi_n &\sim \mathcal{N}(0, 1) \\
 (M_0 < M_1 < N_t)
 \end{aligned}$$

Data-driven modeling

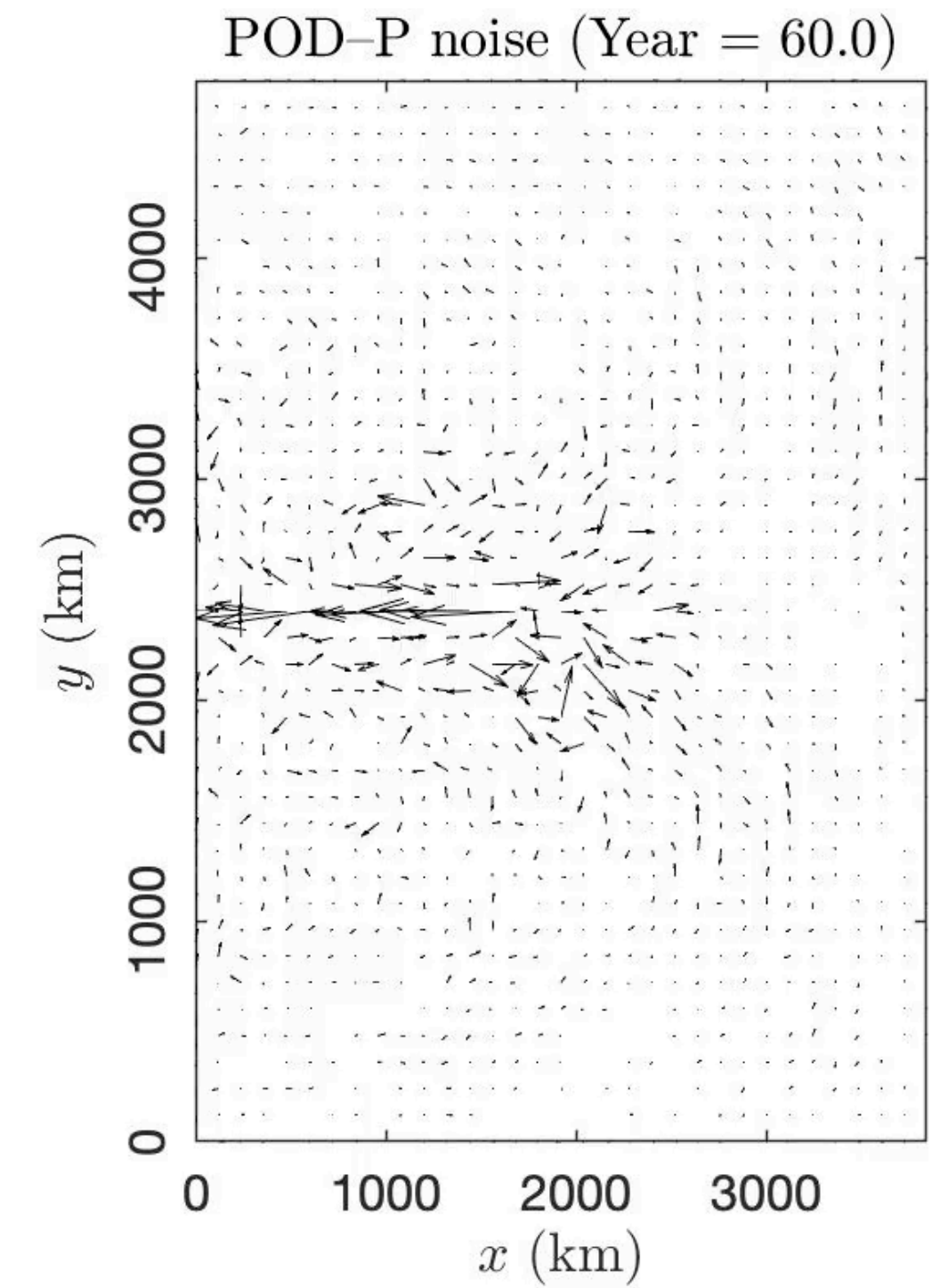
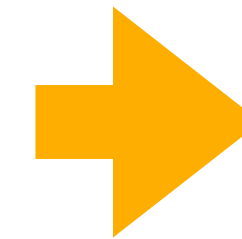
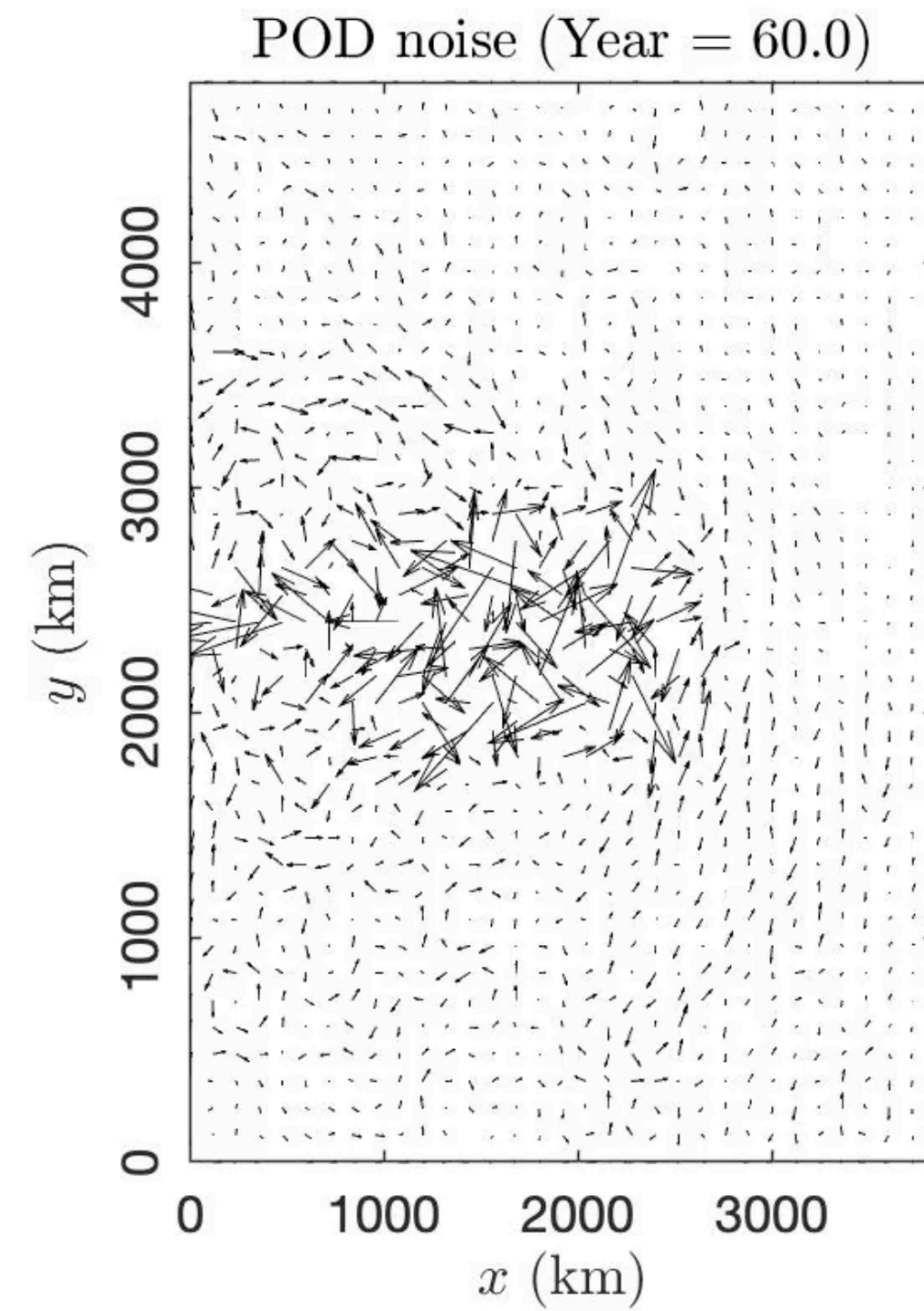
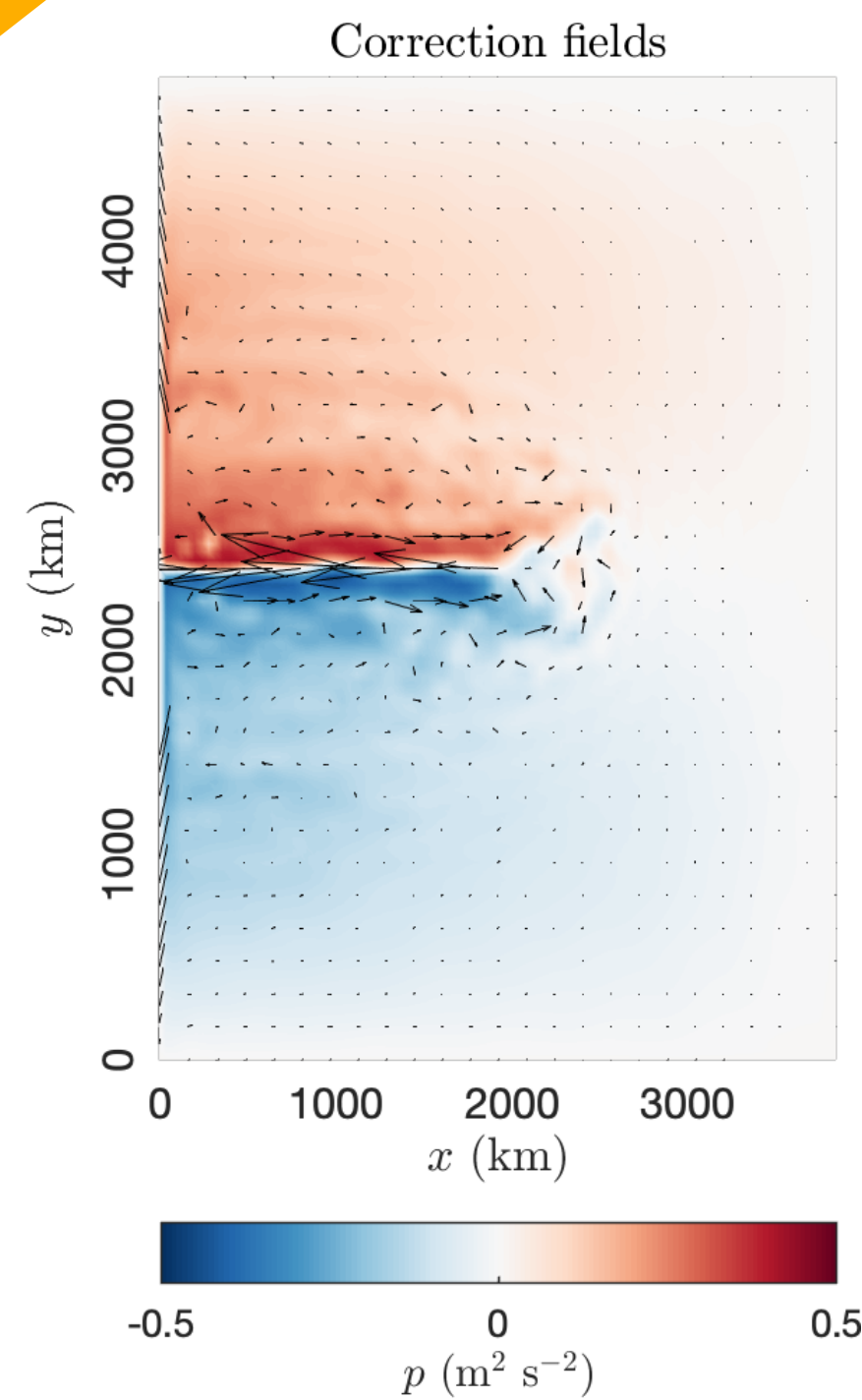
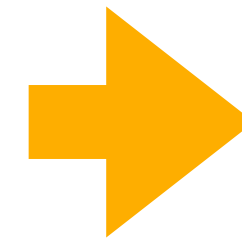
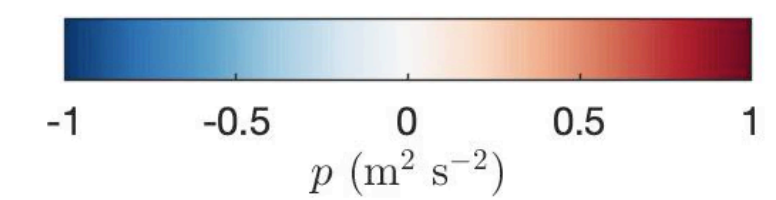
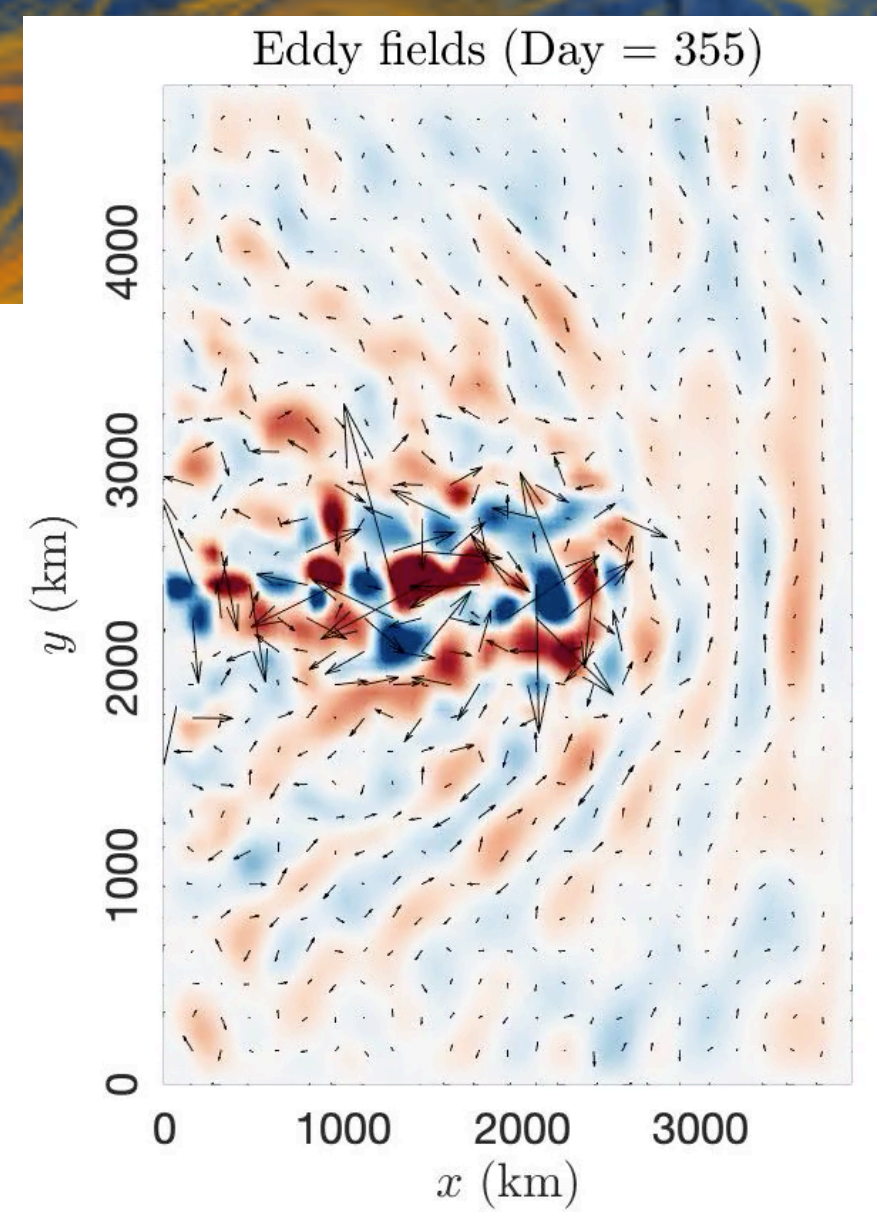
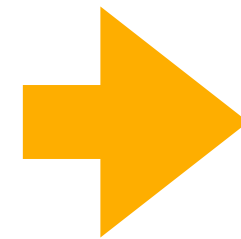
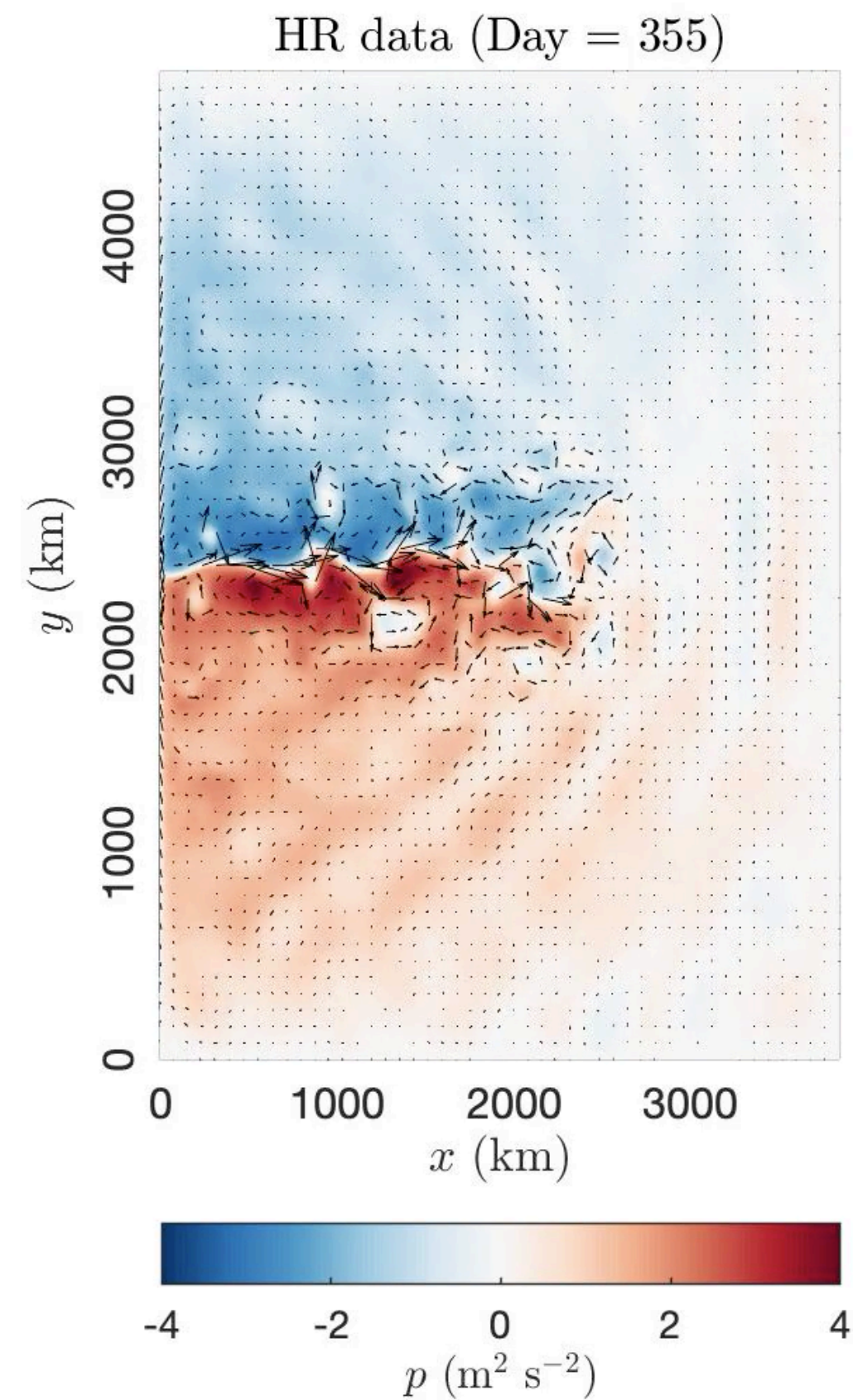
(ii) LU-POD-P

$$\mathbf{P}_k = \mathbf{I} - \frac{\nabla \theta_k (\nabla \theta_k)^T}{\|\nabla \theta_k\|^2}, \quad \theta_k = \frac{f_0}{H_k} (\eta_k - \eta_{k-1})$$

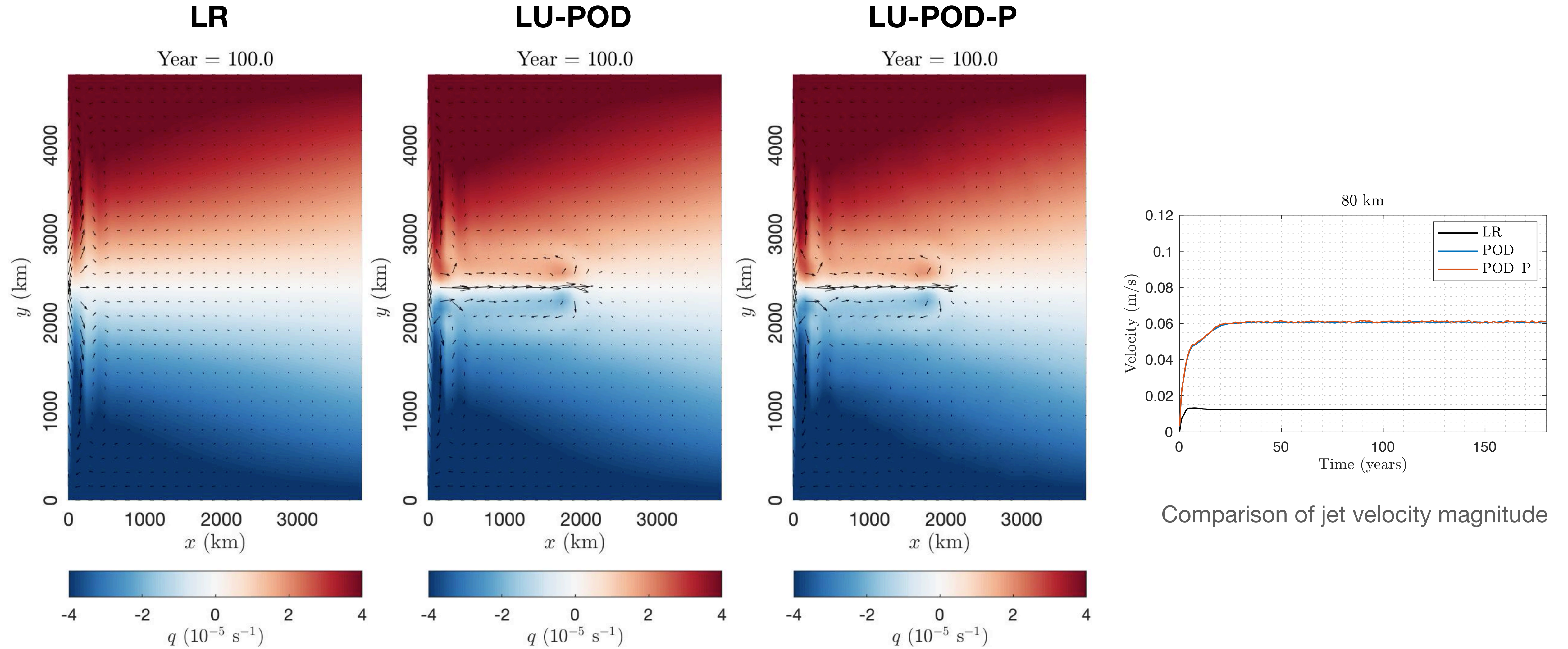
$$\tilde{\sigma}_k \dot{B}_t = \mathbf{P}_k \boxed{\sigma_k \dot{B}_t}, \quad \tilde{a}_k = \mathbf{P}_k \mathbf{a}_k \mathbf{P}_k^T$$

LU-POD

Illustration of noises

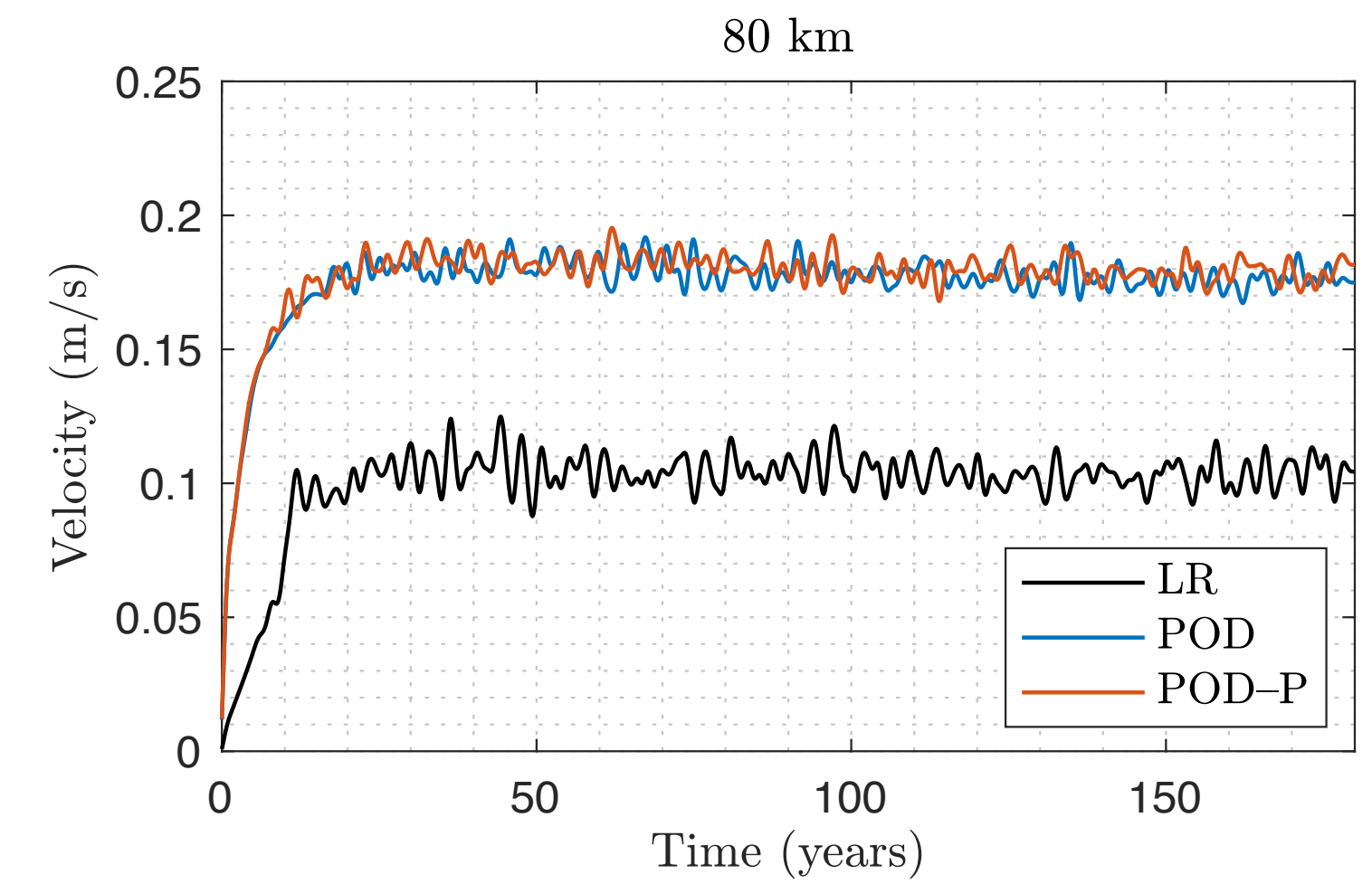
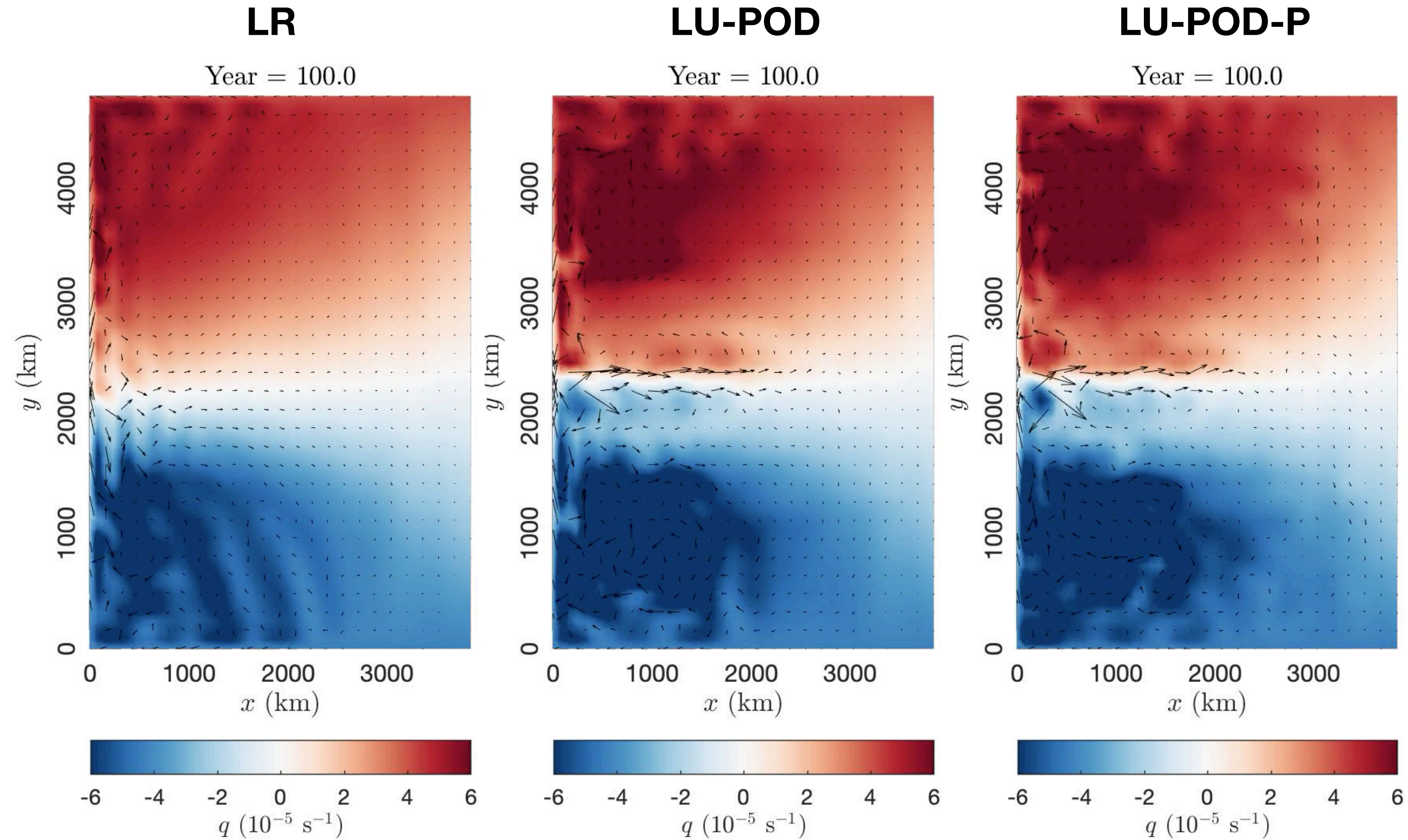


Coarse-resolution simulations



Upper-layer PV ($\Delta x = 80 \text{ km}$, $L_d = [39, 22] \text{ km}$) of Exp.1 (without SST)

Coarse-resolution simulations

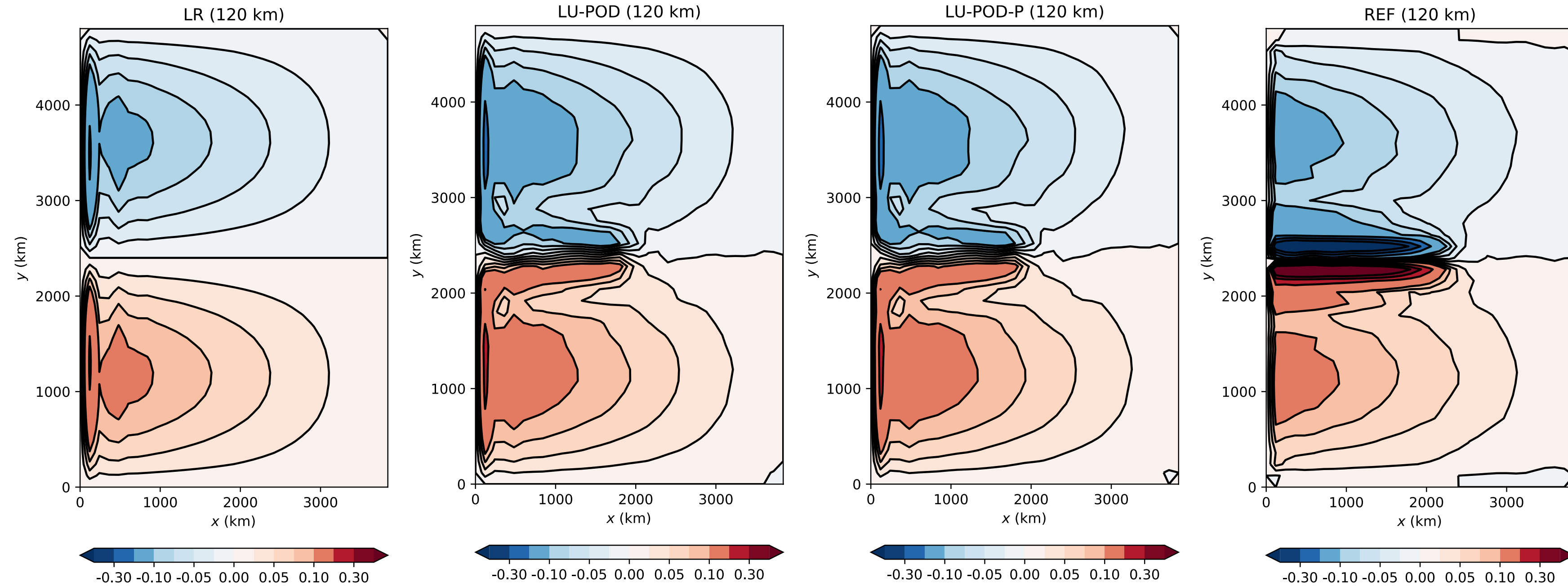


Comparison of jet velocity magnitude

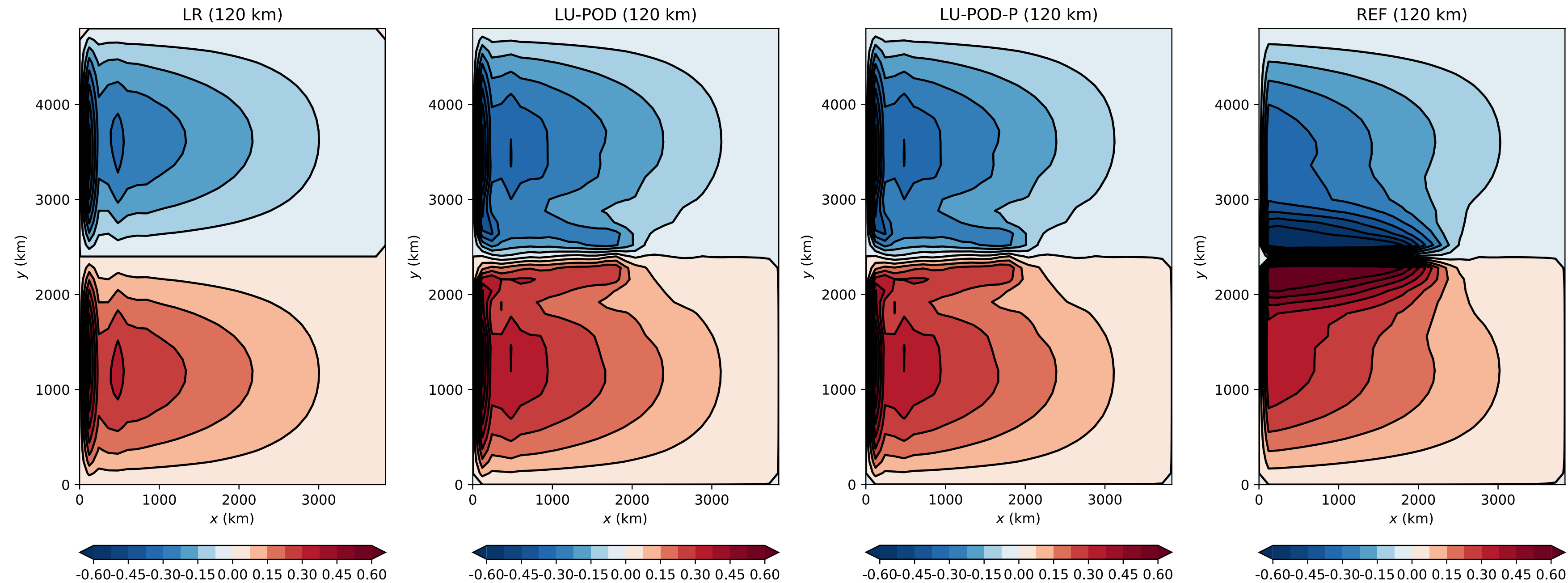
Upper-layer PV ($\Delta x = 80 \text{ km}$, $L_d = [39, 22] \text{ km}$) of **Exp.2** (with SST)

Statistical prediction

**Barotropic
mode**



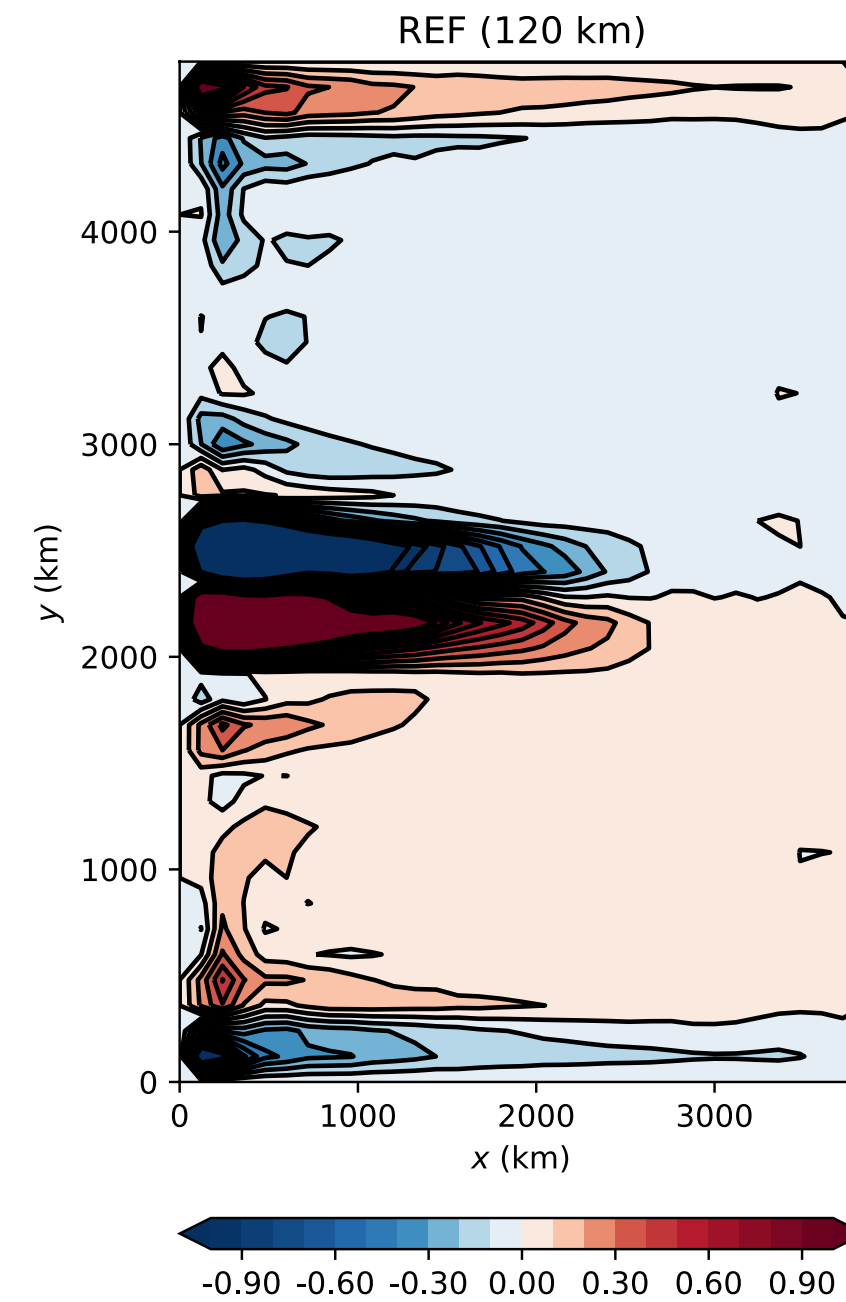
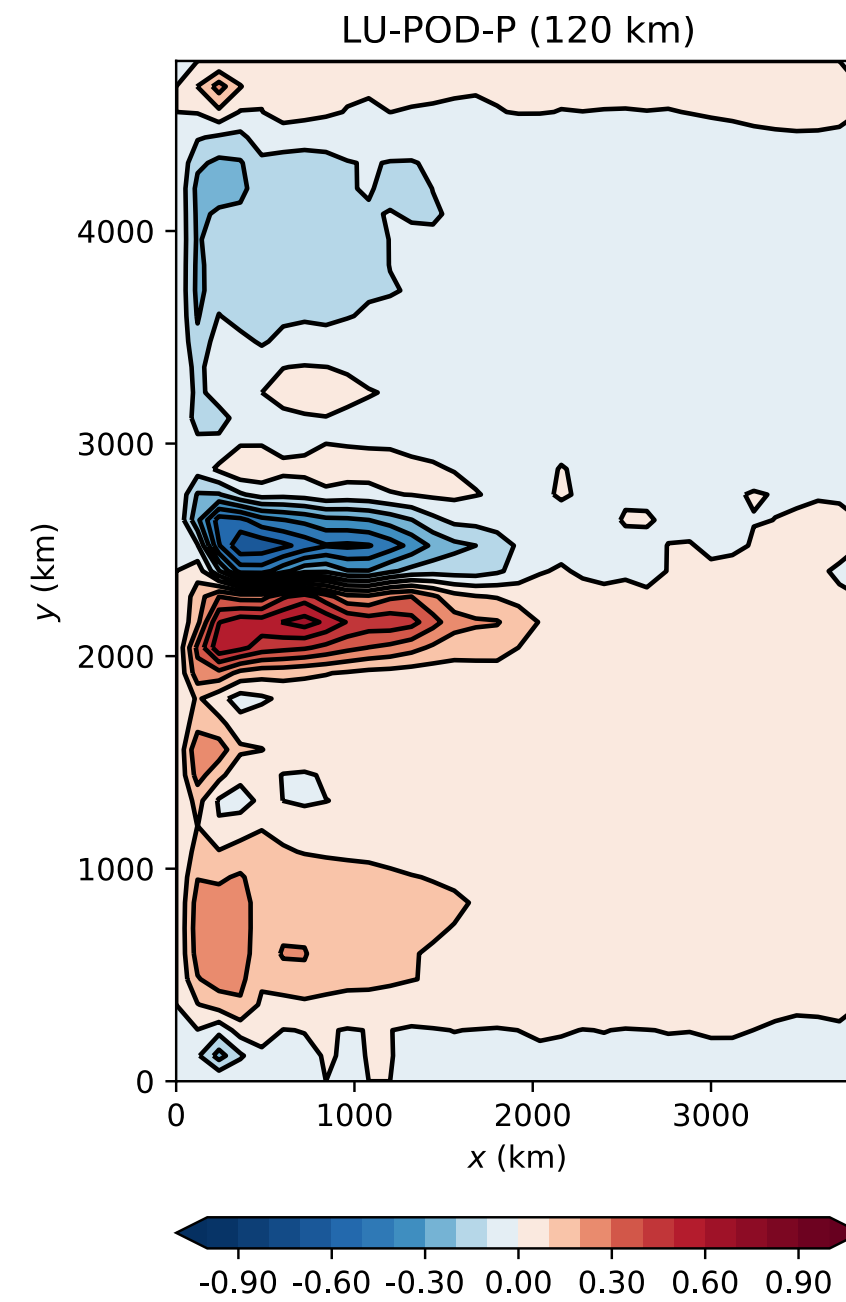
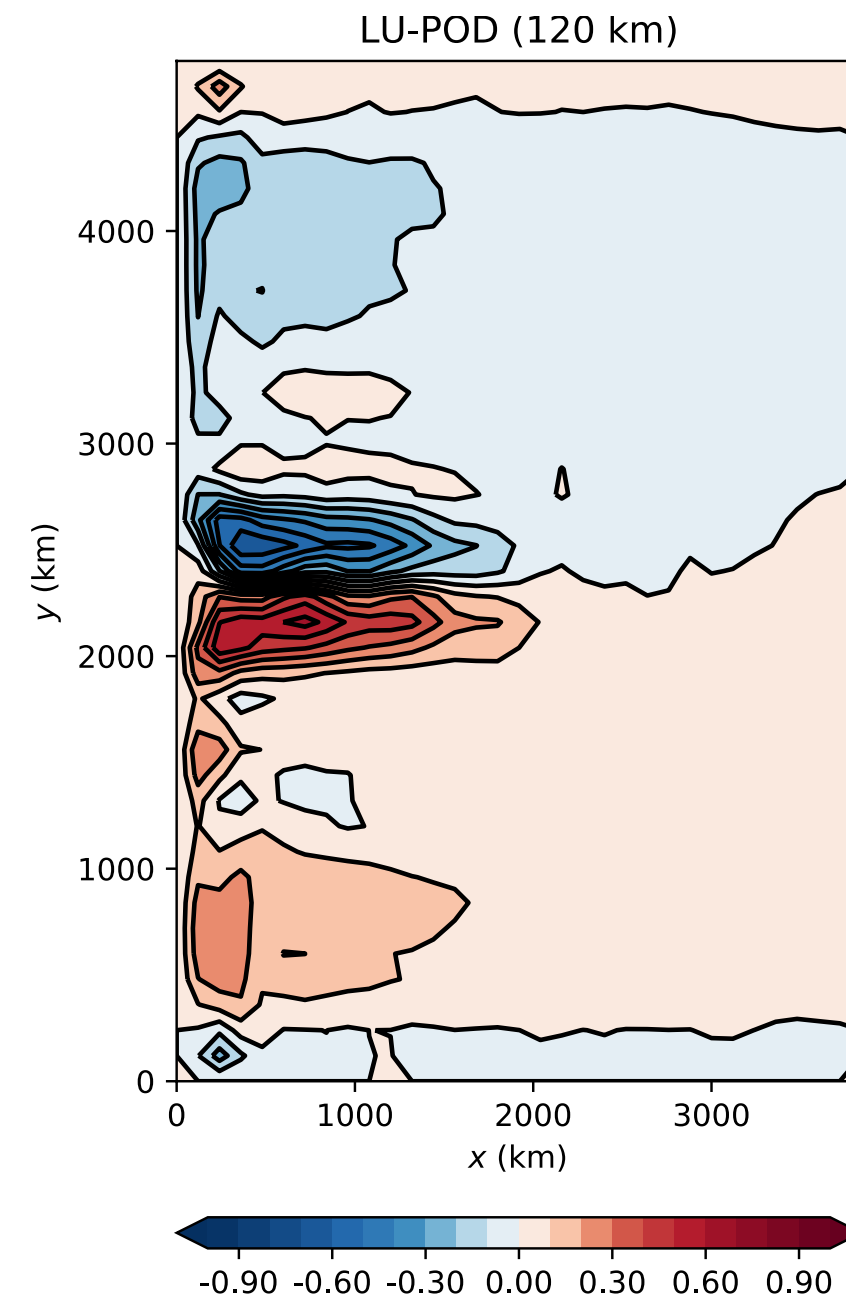
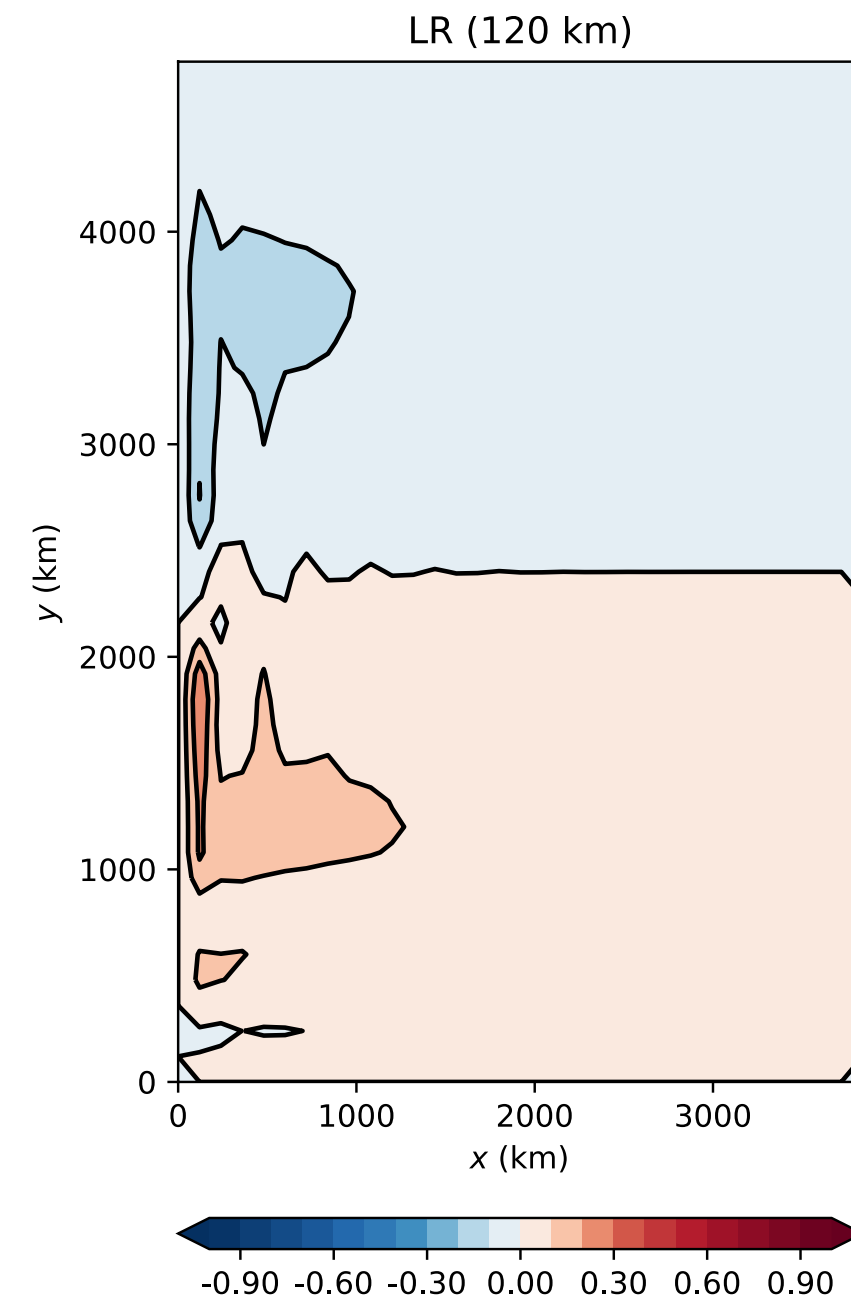
**1st
Baroclinic
mode**



Comparison of
mean (60-180
yrs) contour of
pressure for
coarse-model
(120 km)
simulations
(Exp.1)

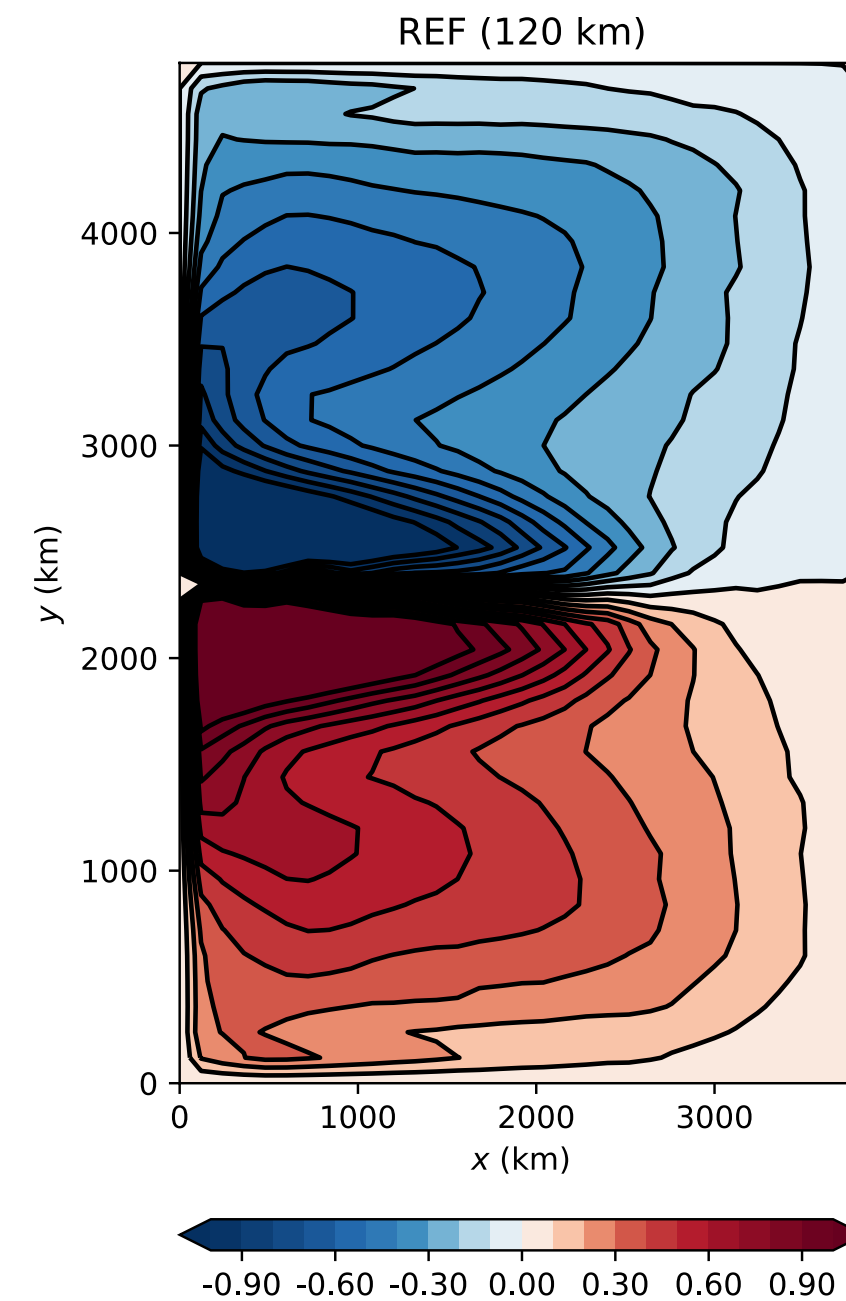
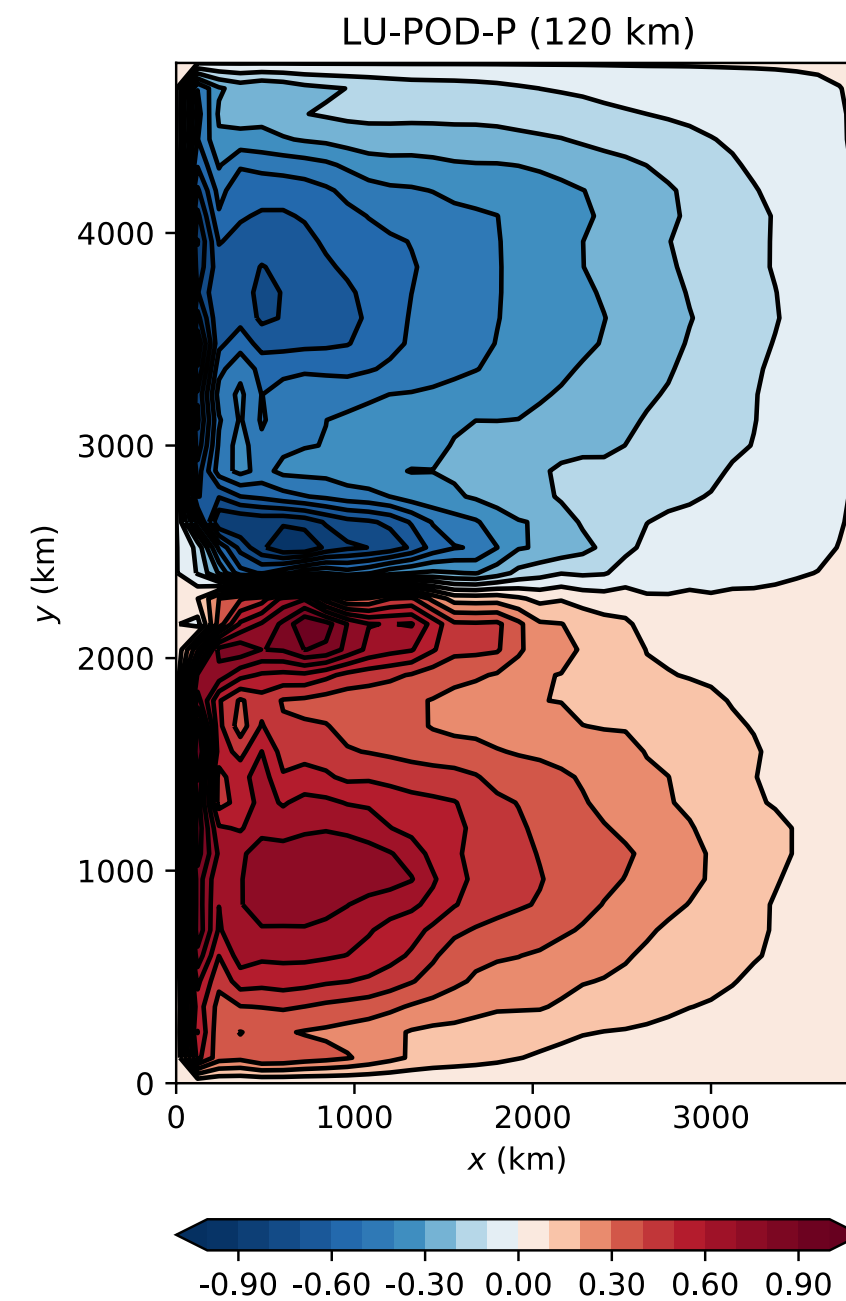
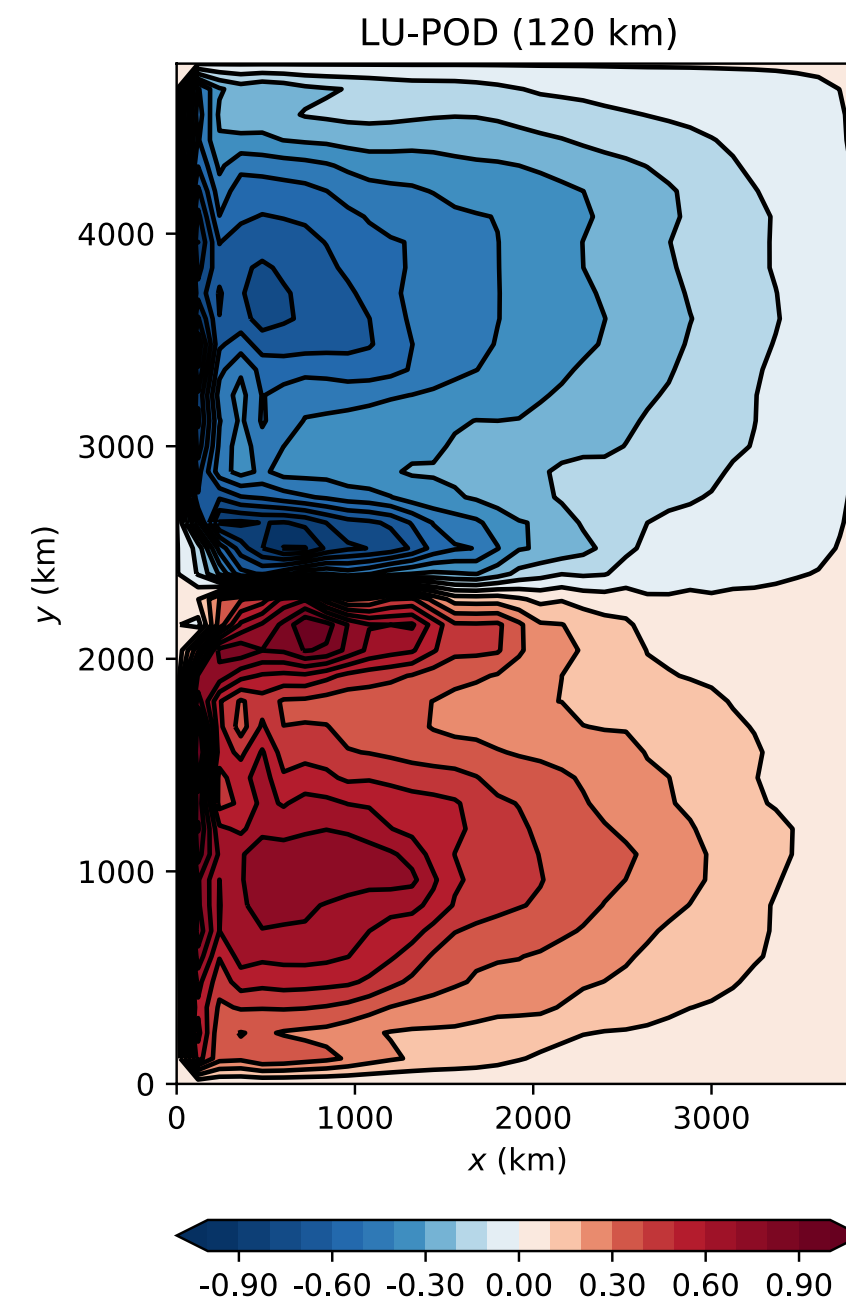
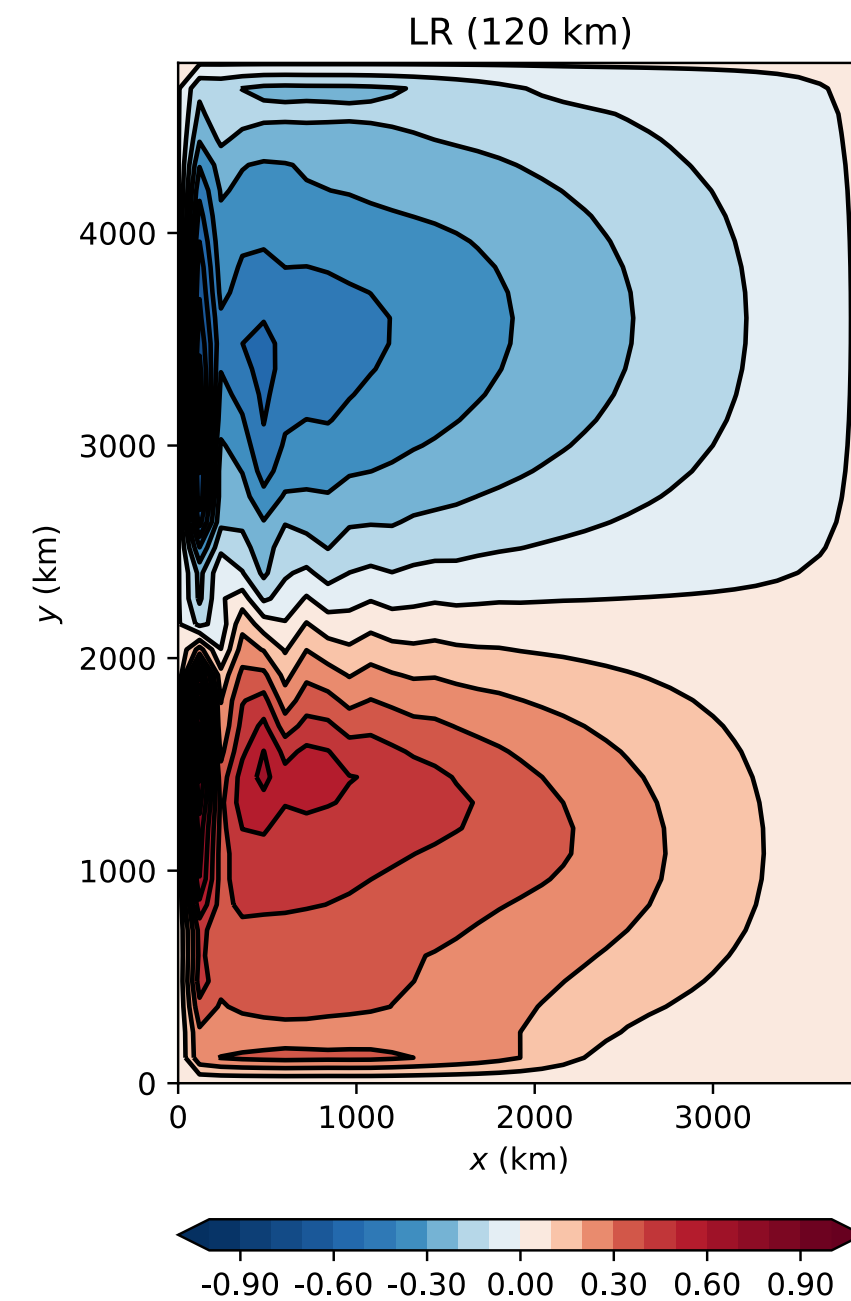
Statistical prediction

**Barotropic
mode**

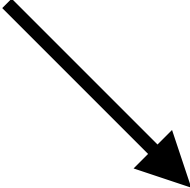
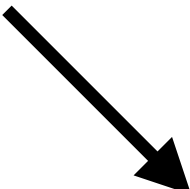
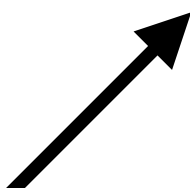
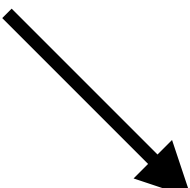
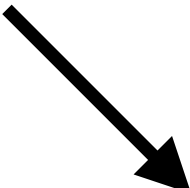


Comparison of
mean (60-180
yrs) contour of
pressure for
coarse-model
(120 km)
simulations
(Exp.2)

**1st
Baroclinic
mode**



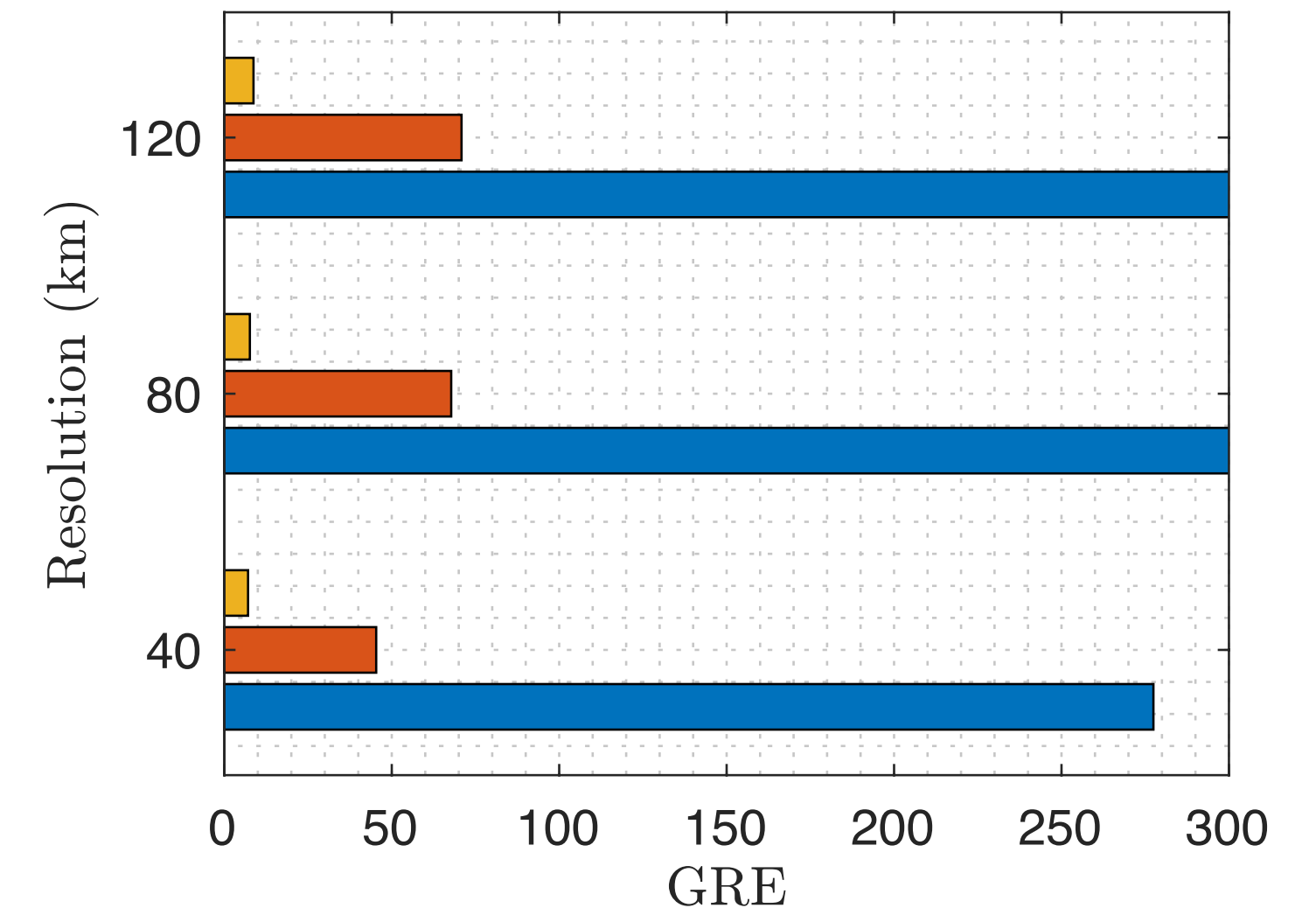
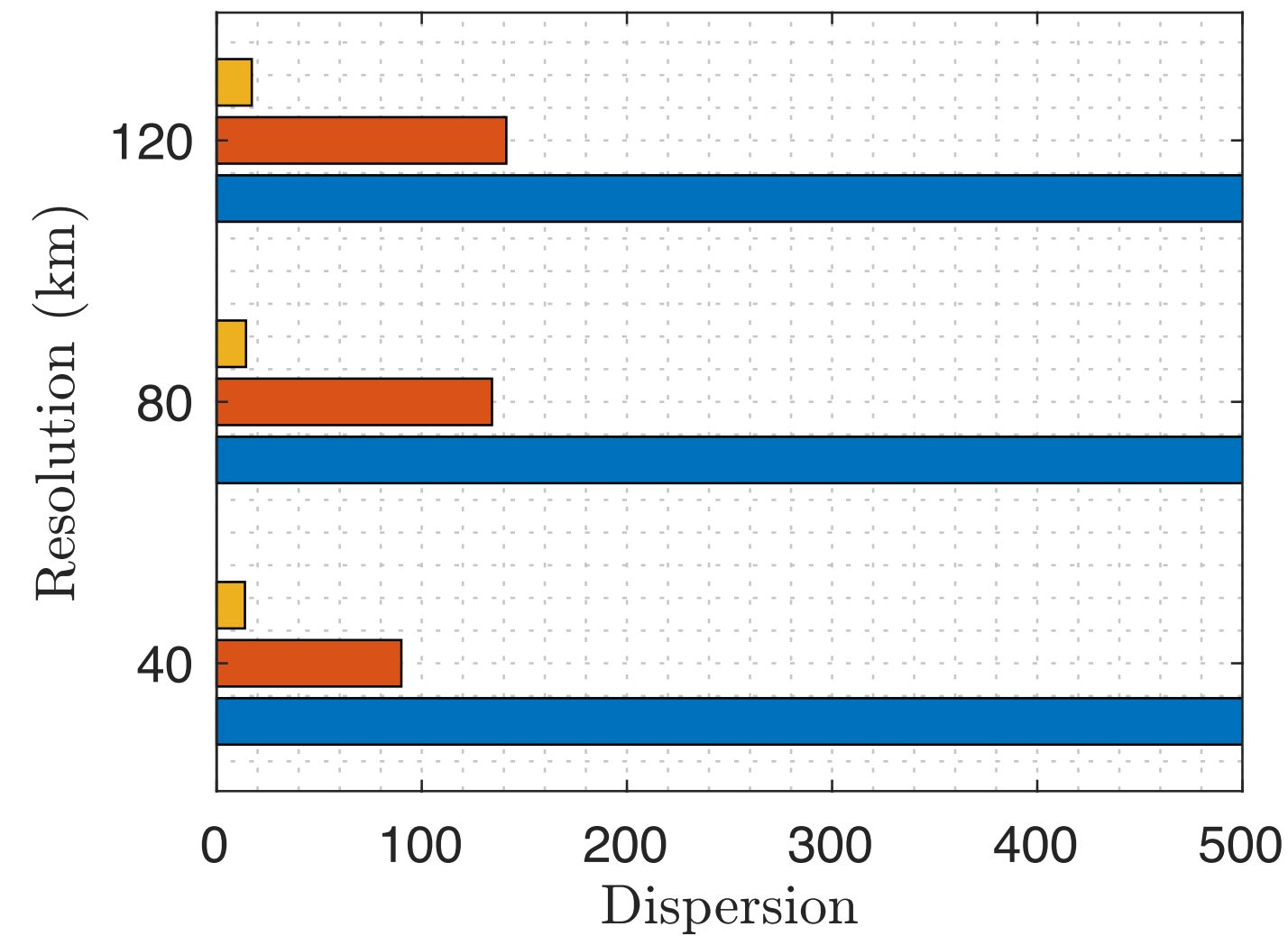
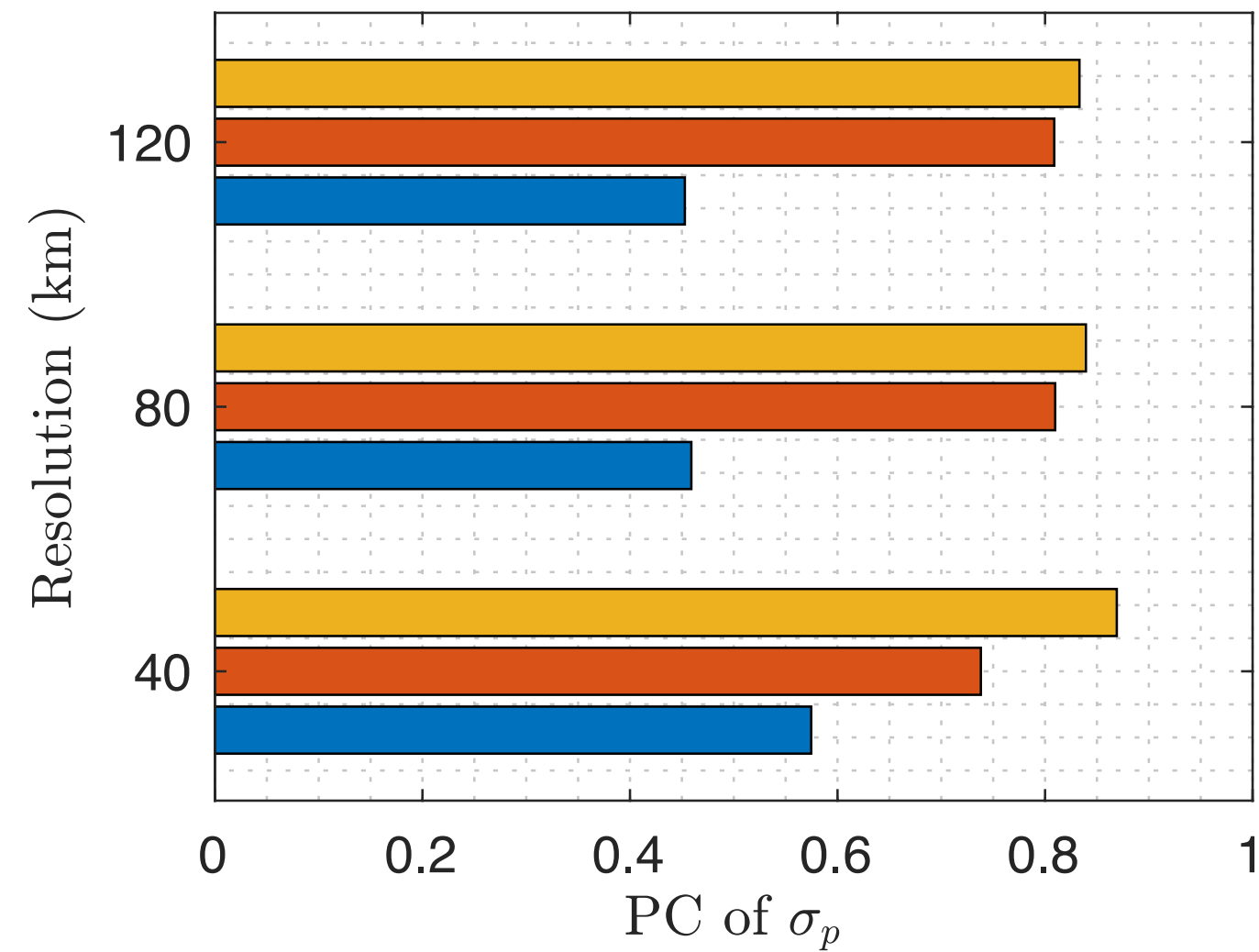
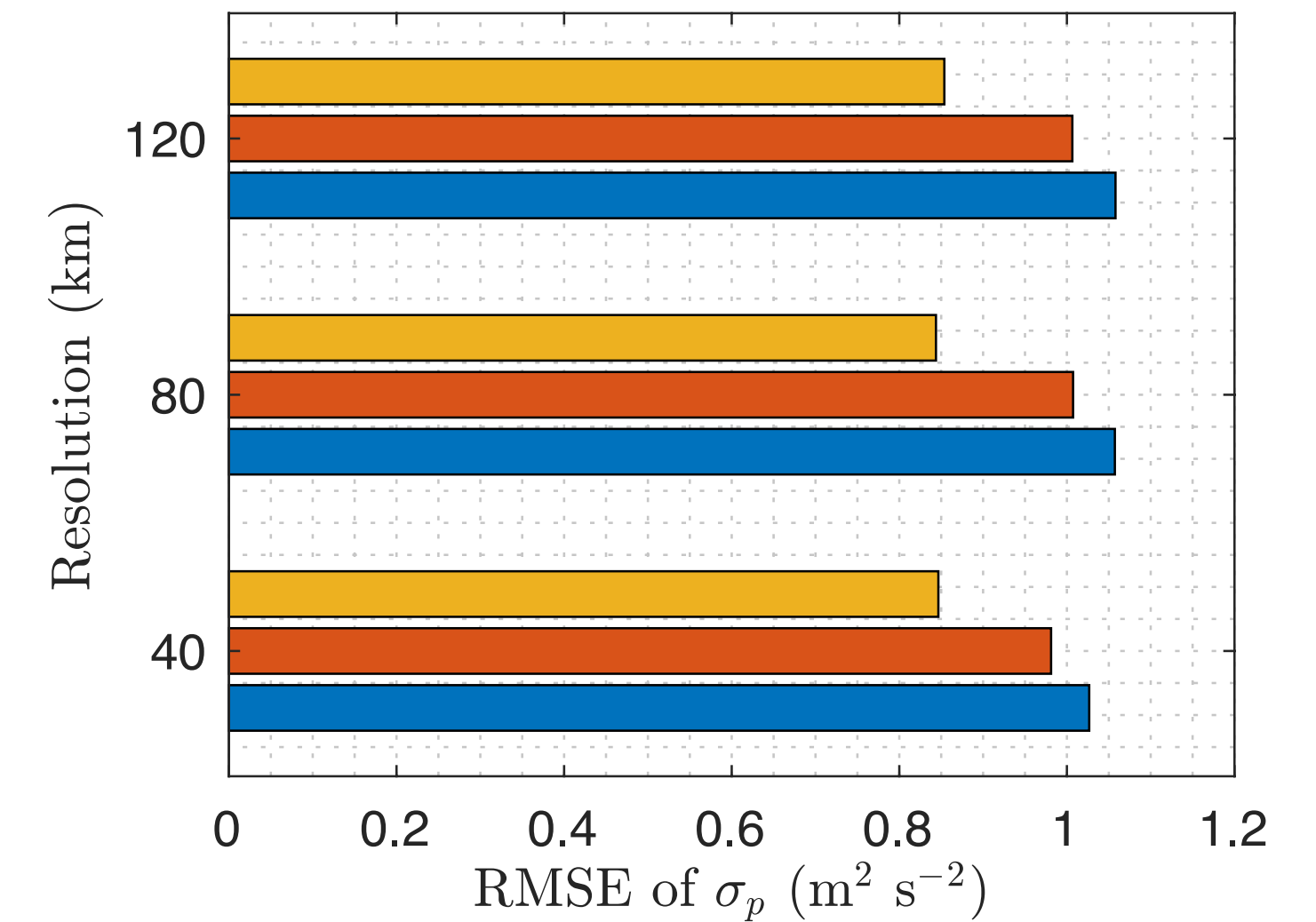
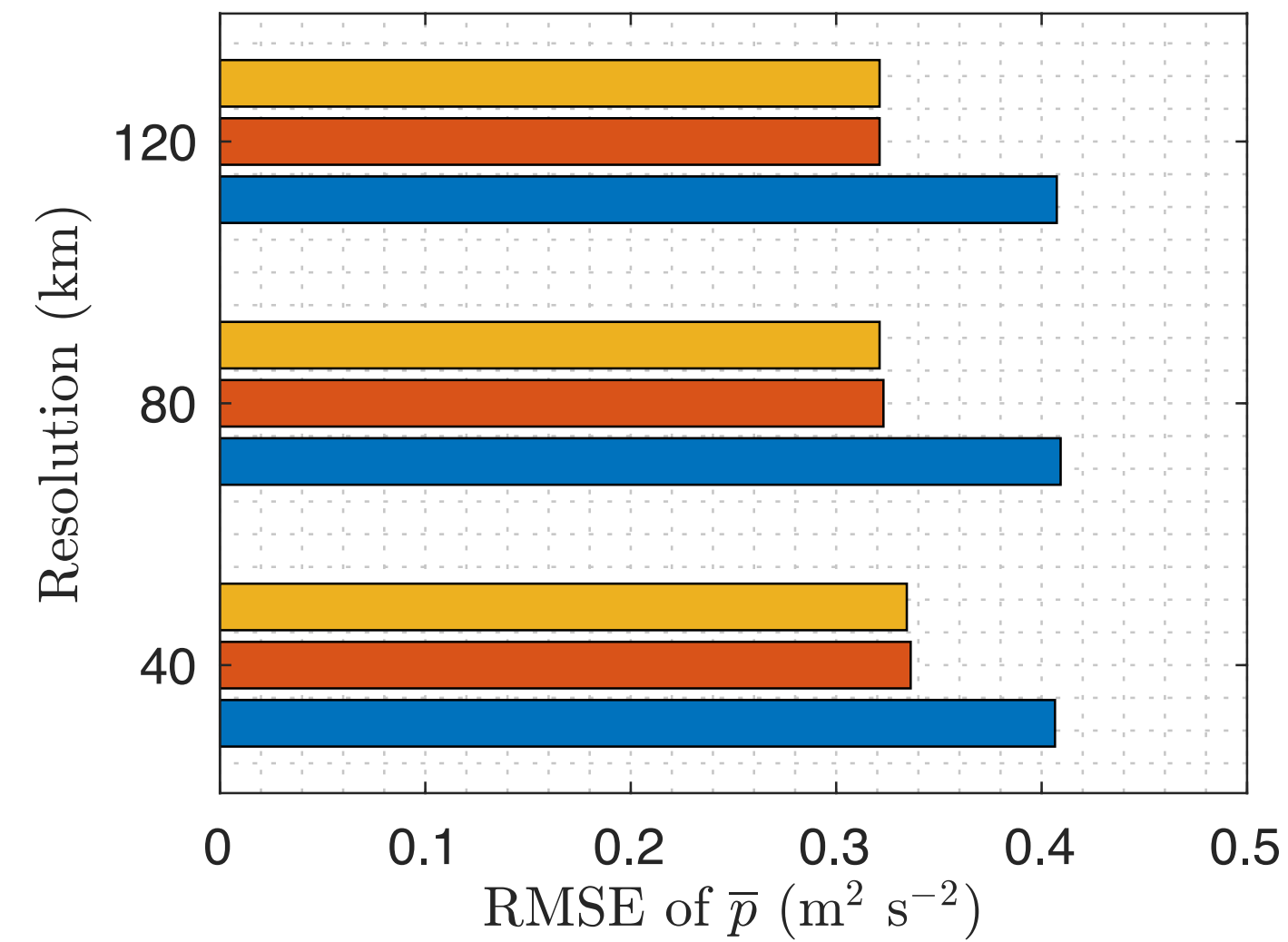
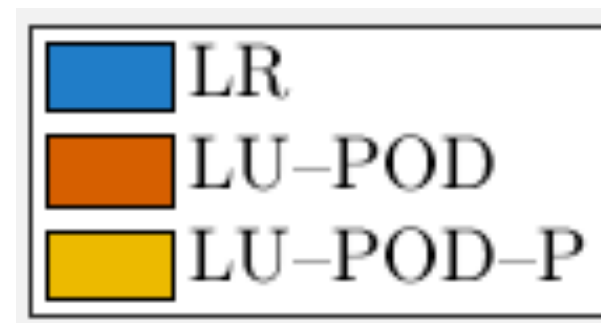
Measures of statistics

Measures	Values	Accuracy
RMSE of $\bar{p}_{\text{MOD}} = \ \bar{p}_{\text{MOD}} - \bar{p}_{\text{REF}}\ _A$		+
RMSE of $\sigma_{\text{MOD}} = \ \sigma_{\text{MOD}} - \sigma_{\text{REF}}\ _A$, $\sigma = \overline{(p - \bar{p})^2}$		+
$\text{PC} = \frac{\ \sigma_{\text{REF}} \sigma_{\text{MOD}}\ _A^2}{\ \sigma_{\text{REF}}^2\ _A \ \sigma_{\text{MOD}}^2\ _A}$		+
Dispersion = $\frac{1}{ A } \int \int \left(\frac{\sigma_{\text{REF}}^2}{\sigma_{\text{MOD}}^2} - 1 - \log \left(\frac{\sigma_{\text{REF}}^2}{\sigma_{\text{MOD}}^2} \right) \right) \text{d}A$		+
$\text{GRE} = \frac{1}{2} \left\ \frac{\bar{p}_{\text{REF}} - \bar{p}_{\text{MOD}}}{\sigma_{\text{REF}}} \right\ _A^2 + \frac{1}{2} \text{Dispersion}$		+

$$\|f\|_A = \left(\frac{1}{|A|} \int \int f^2 \text{d}A \right)^{1/2}$$

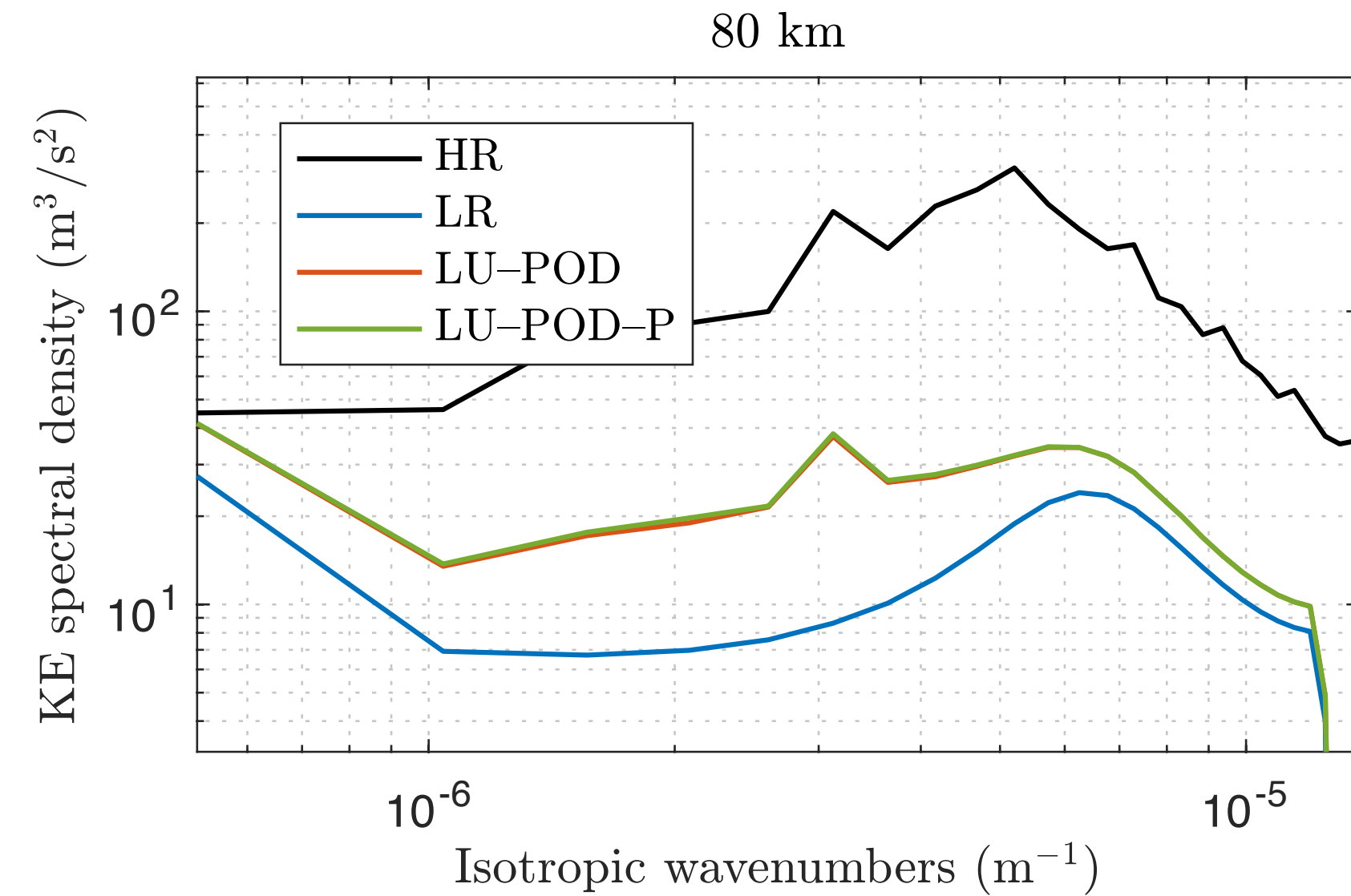
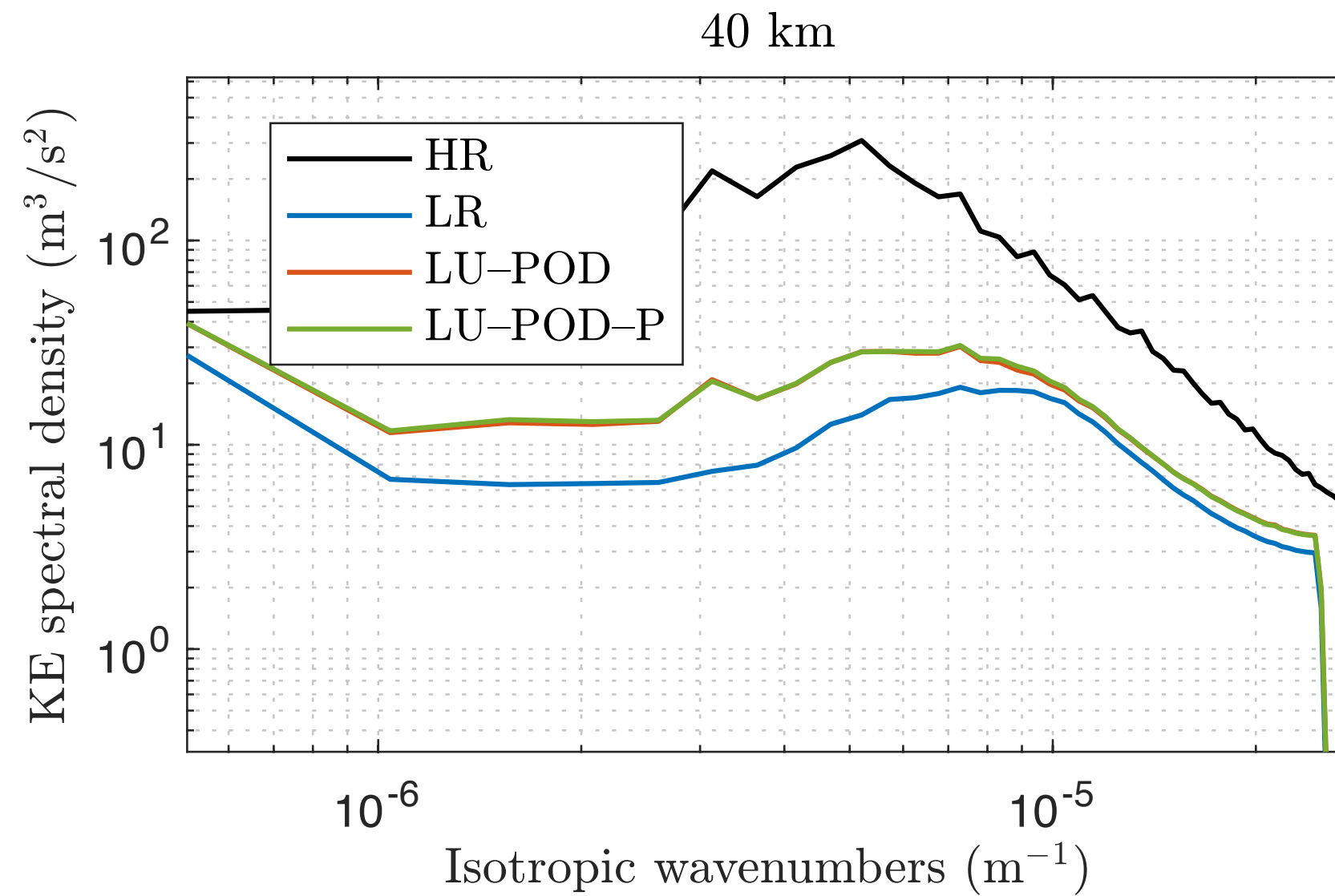
Statistical prediction

Comparison of statistical measures (integrated vertically) for pressures provided by different coarse models (Exp.2)



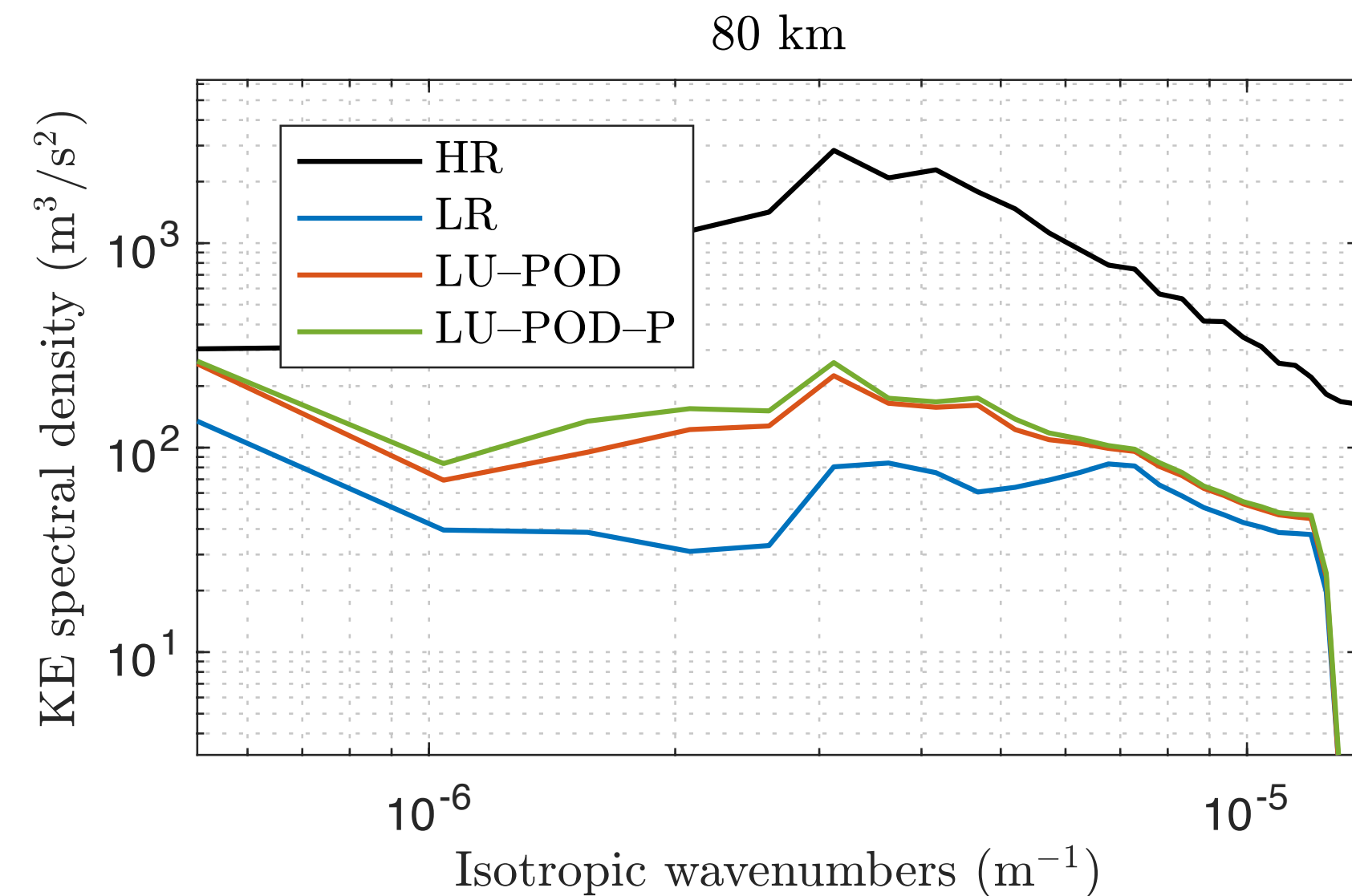
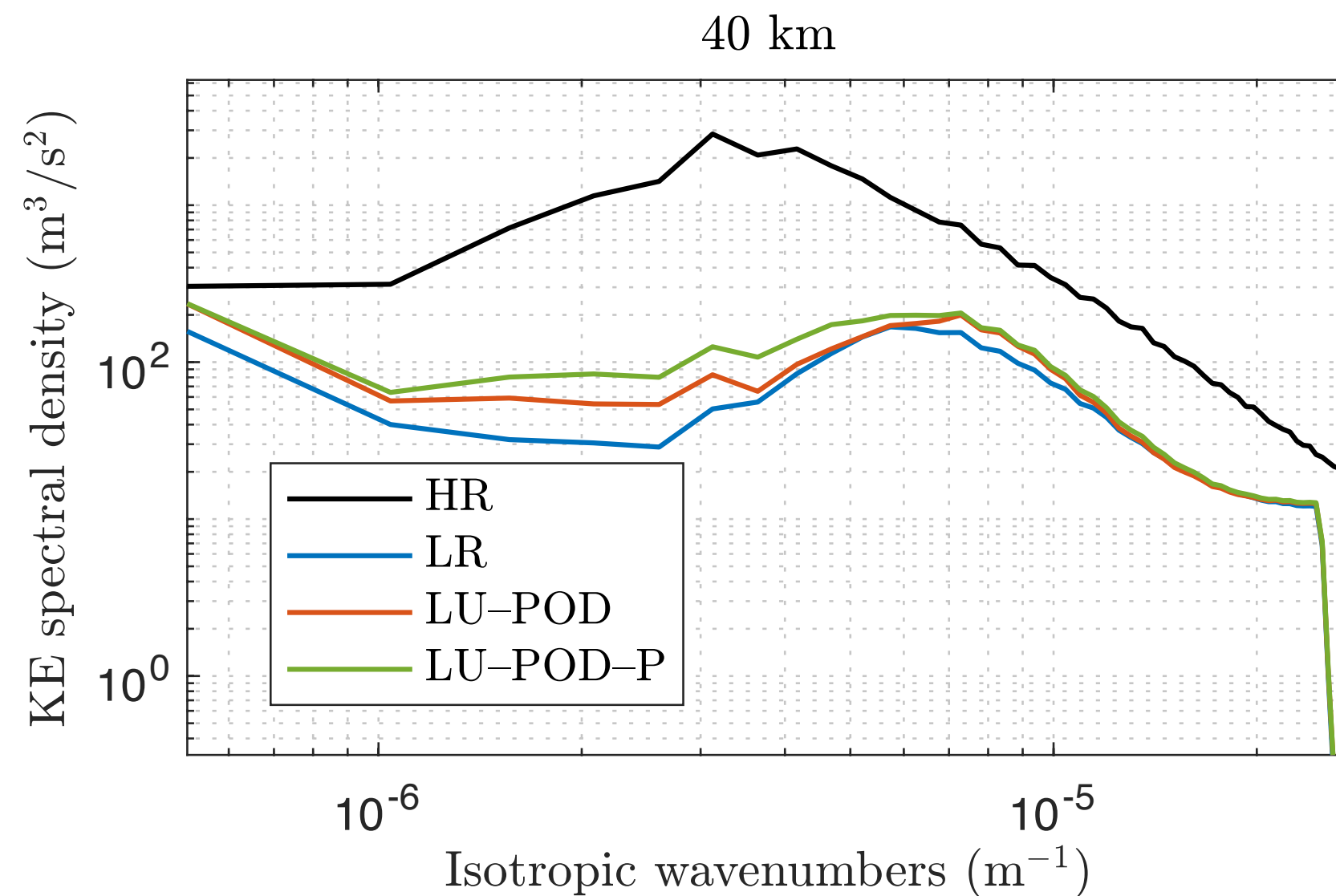
Energy analysis

**Exp.1
(without SST)**



**Comparison of
KE spectral
density
averaged in
time (60-75 yrs)
and in layers
for different
coarse models**

**Exp.2
(with SST)**

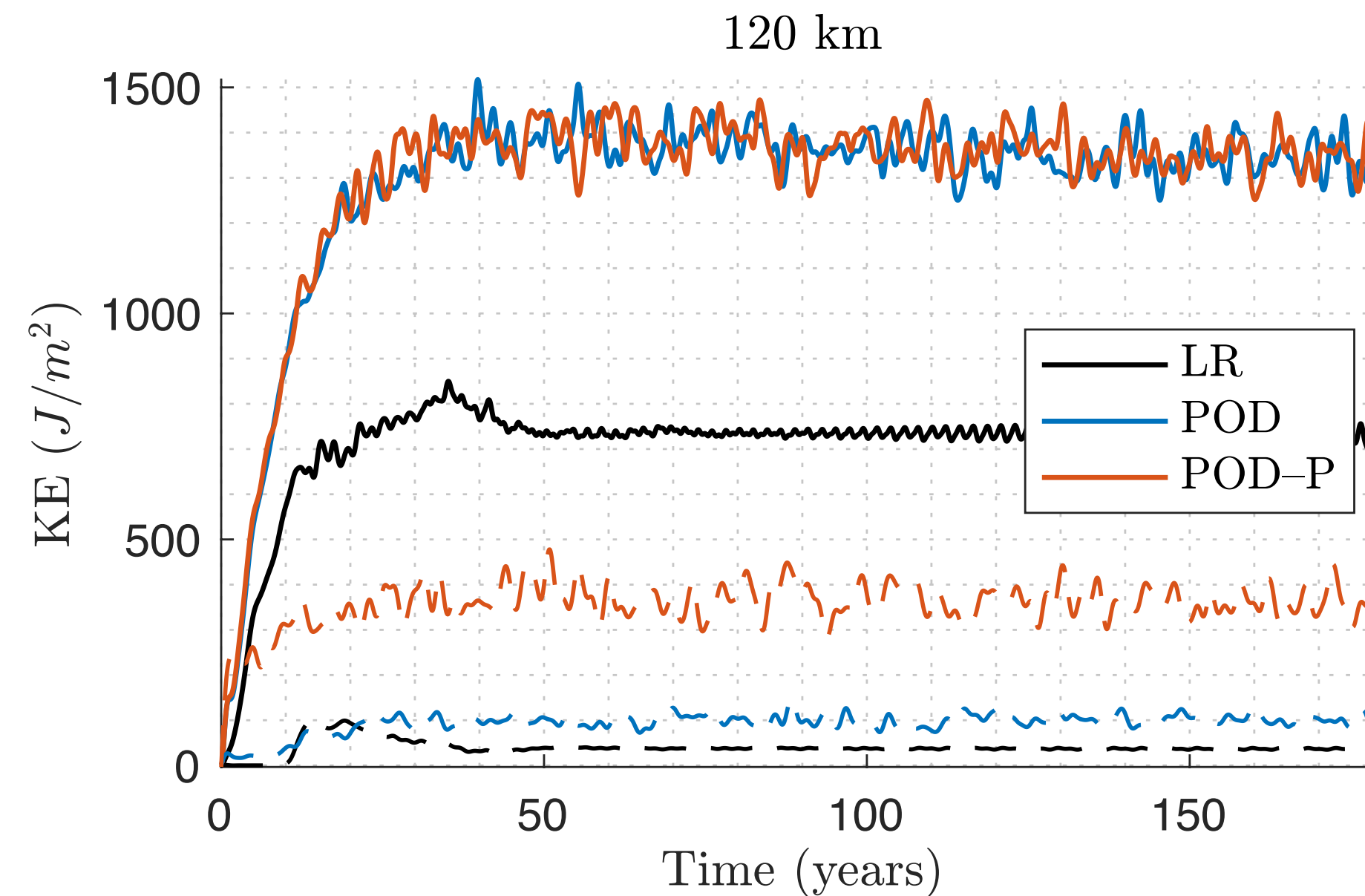
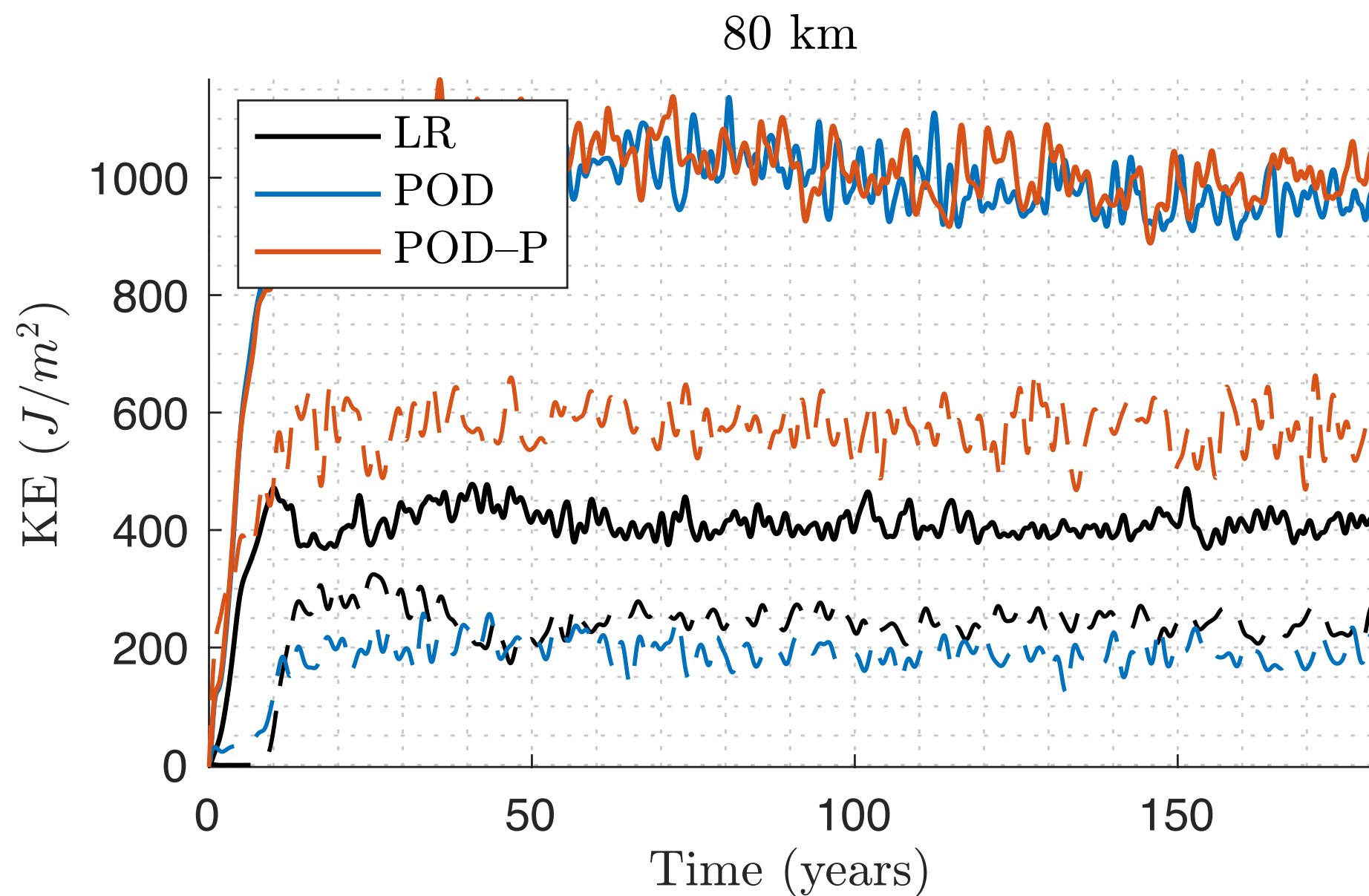


Energy analysis

- KE decomposition

$$\mathbf{u}_k = \overline{\mathbf{u}}_k + \mathbf{u}'_k \quad \text{Low-pass filtering}$$

$$\text{EKE}_k = \underbrace{\frac{\rho_0 H_k}{2} \|\overline{\mathbf{u}}_k\|_A^2}_{\text{Standing EKE}} + \underbrace{\frac{\rho_0 H_k}{2} \|\mathbf{u}'_k\|_A^2}_{\text{Transient EKE}}$$



Comparison of EKE
(integrated over layers) for different coarse models
(Solid lines — standing EKE, Dashed lines — transient EKE)

Energy analysis

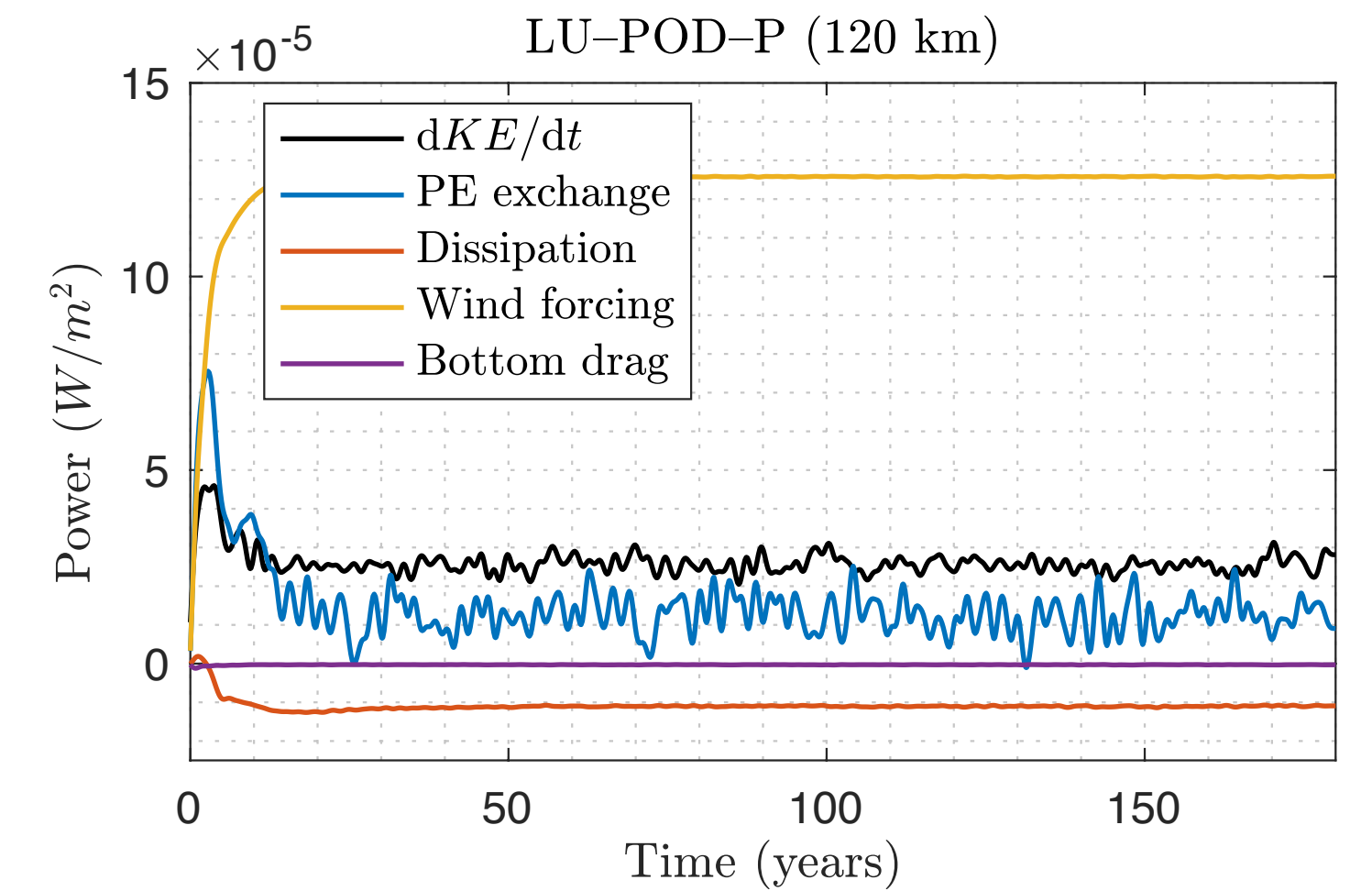
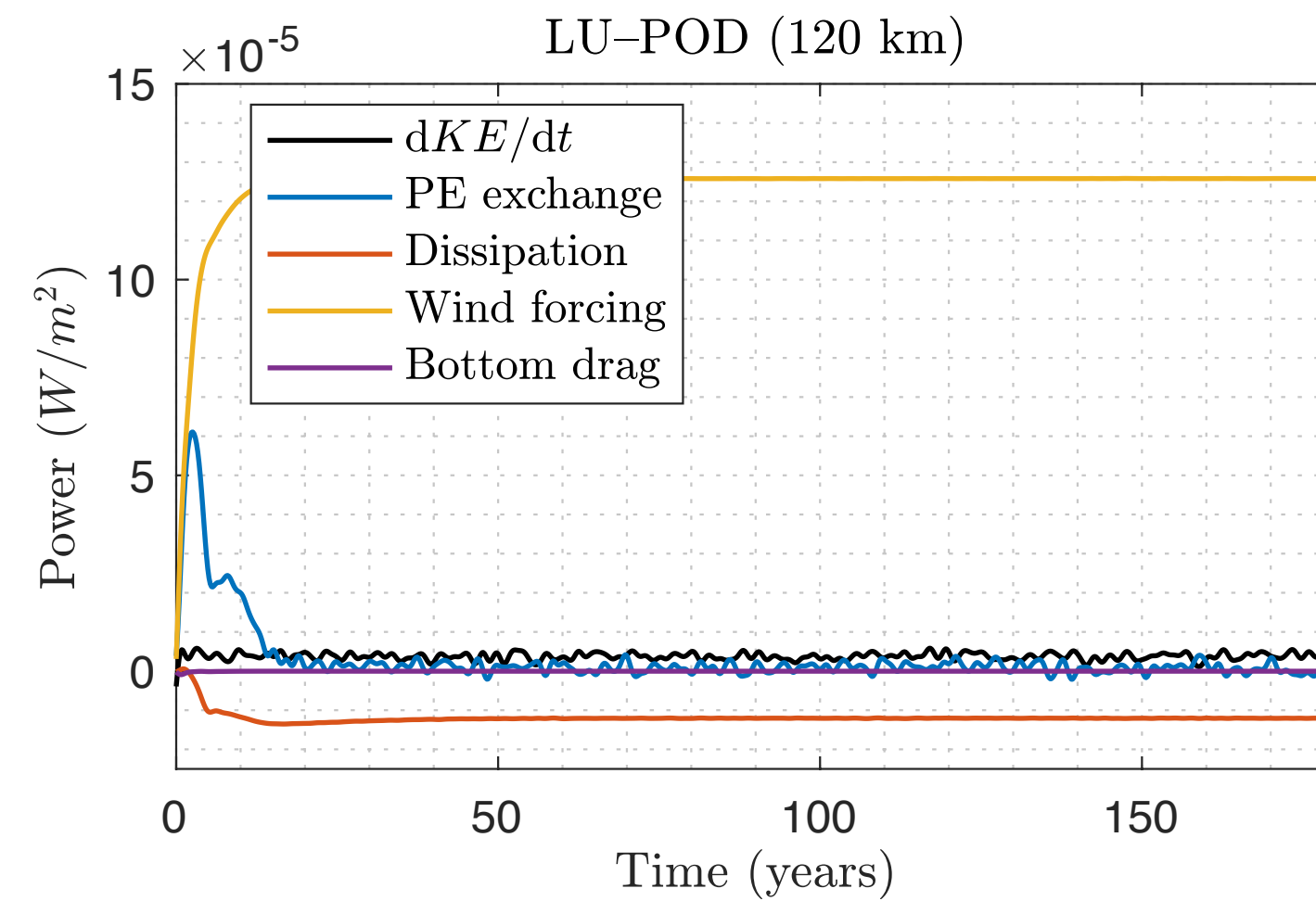
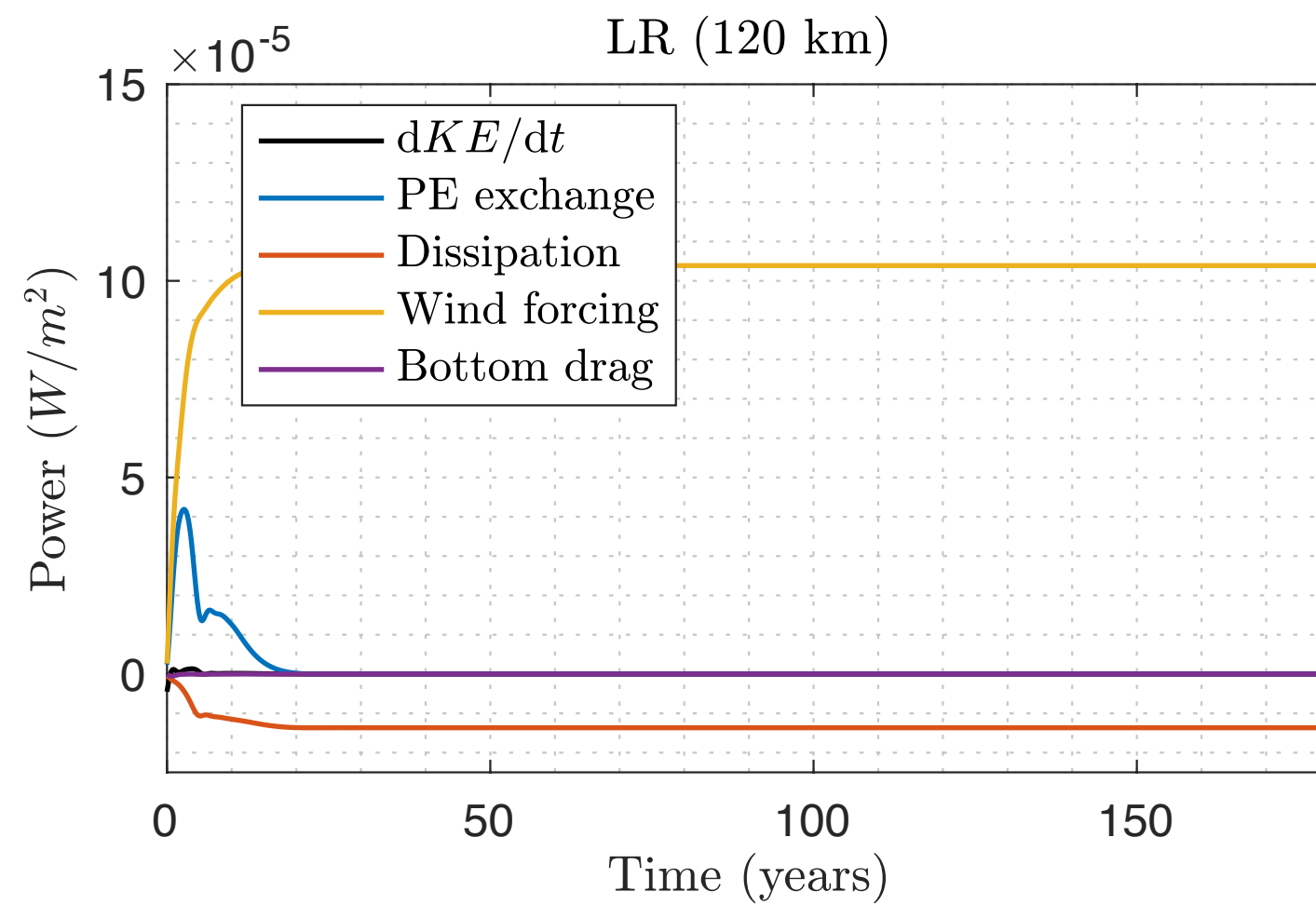
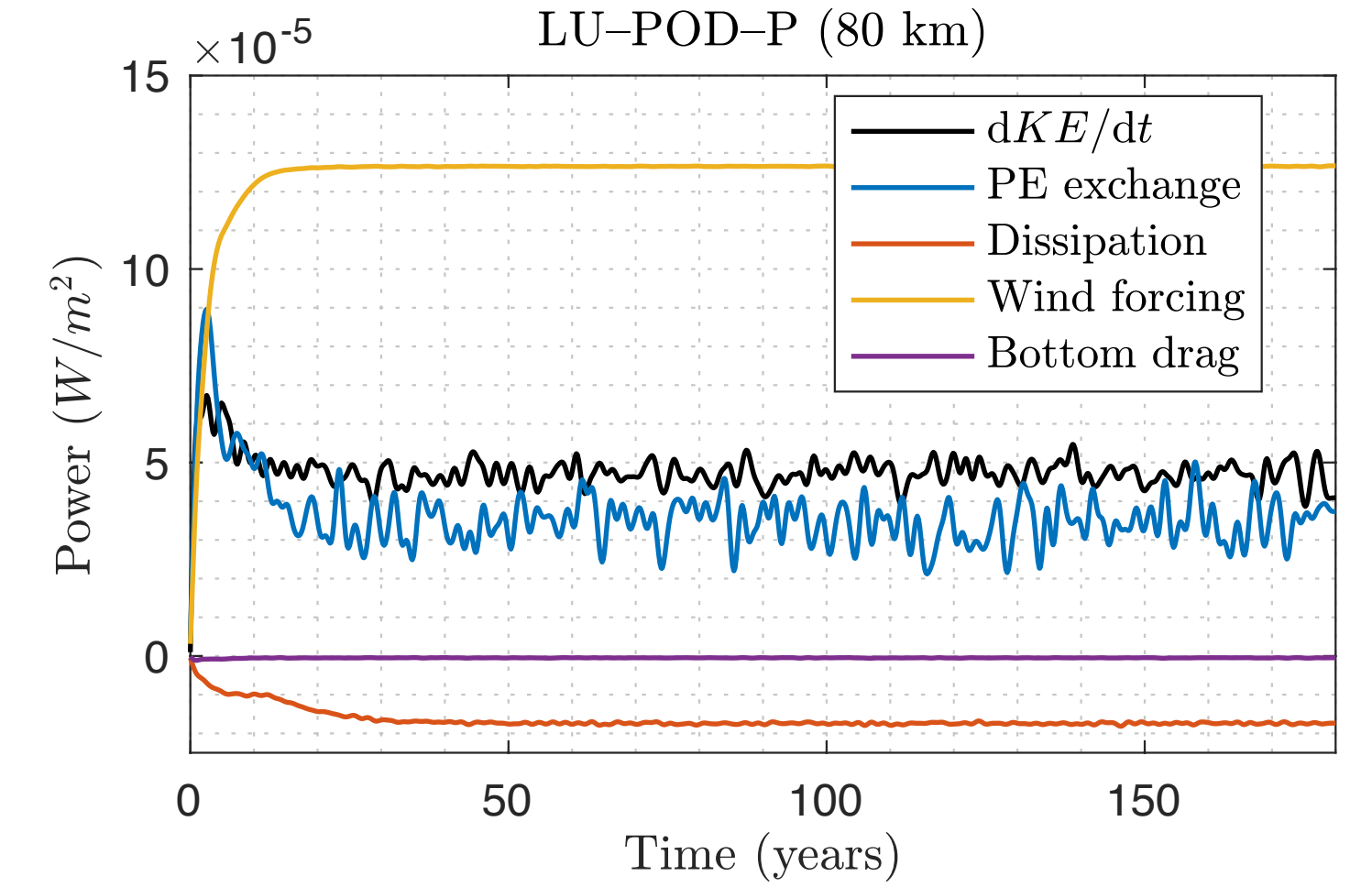
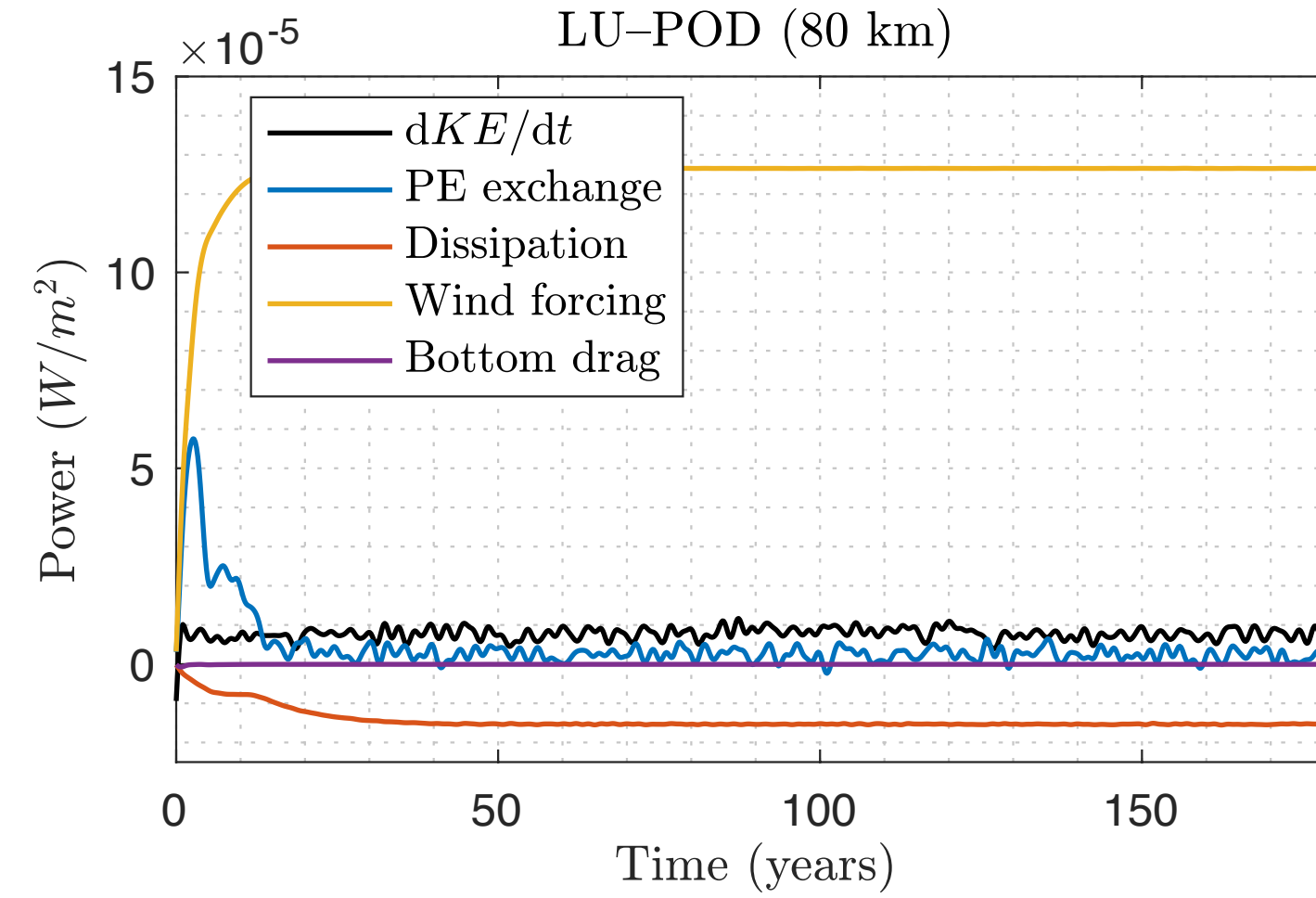
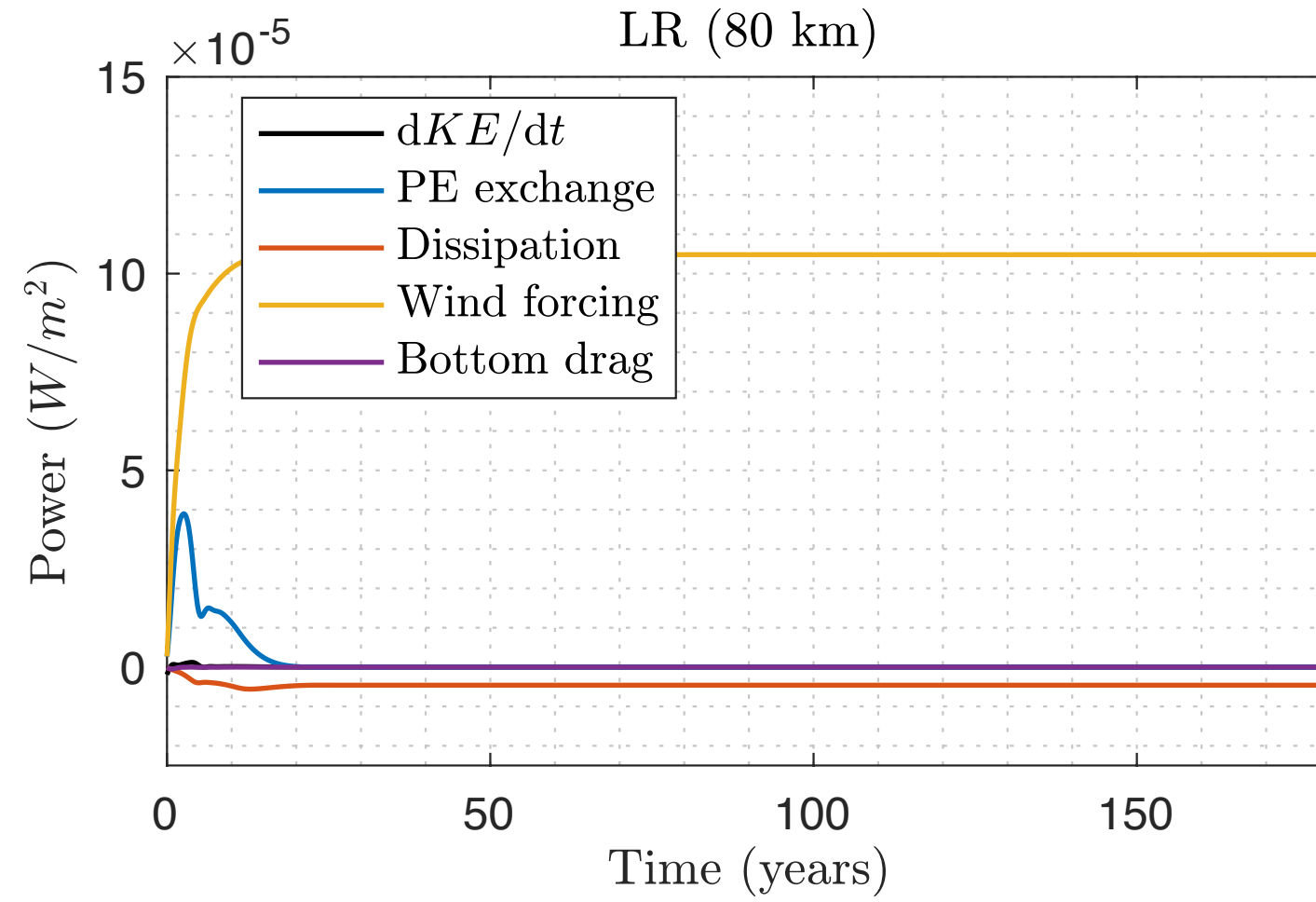
- KE contributions

$$\begin{aligned}
 & \text{KE} \quad \partial_t \sum_{k=1}^N \boxed{\frac{\rho_0 H_k}{2} \|\mathbf{u}_k\|_A^2} = -\partial_t \sum_{k=1}^{N-1} \boxed{\frac{\rho_0 g'_k}{2} \|\eta_k\|_A^2} - \sum_{k=1}^{N-1} \boxed{\rho_0 g'_k \langle \eta_k, w_k \rangle_A} \quad \text{Buoyancy forcing} \\
 & \quad \quad \quad \text{Wind forcing} \quad + \boxed{\rho_0 \langle \mathbf{u}_1, \boldsymbol{\tau} \rangle_A} - \boxed{\frac{\rho_0 f_0 \delta_{ek}}{2} \|\mathbf{u}_N\|_A^2} \quad \text{Bottom drag} \\
 & \quad \quad \quad + \sum_{k=1}^N \boxed{\rho_0 H_k \langle \mathbf{u}_k, A_2 \nabla^2 \mathbf{u}_k - A_4 \nabla^4 \mathbf{u}_k \rangle_A} \\
 & \quad \quad \quad \text{Dissipation}
 \end{aligned}$$

(= 0 in Exp.1)

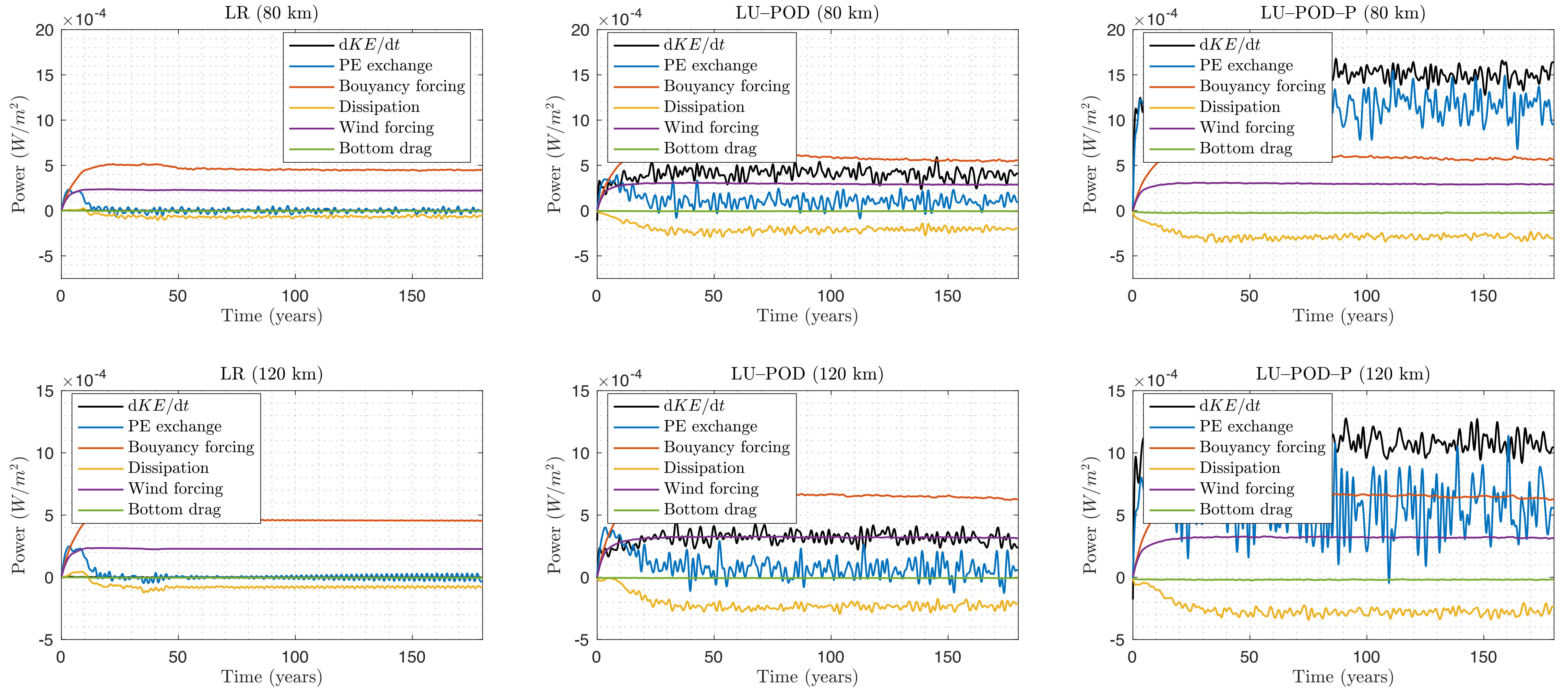
$$\langle f, g \rangle_A = \frac{1}{|A|} \int \int f g \, dA$$

Energy analysis



Comparison of contributions to the rate of KE for different coarse models (Exp.1)

Energy analysis

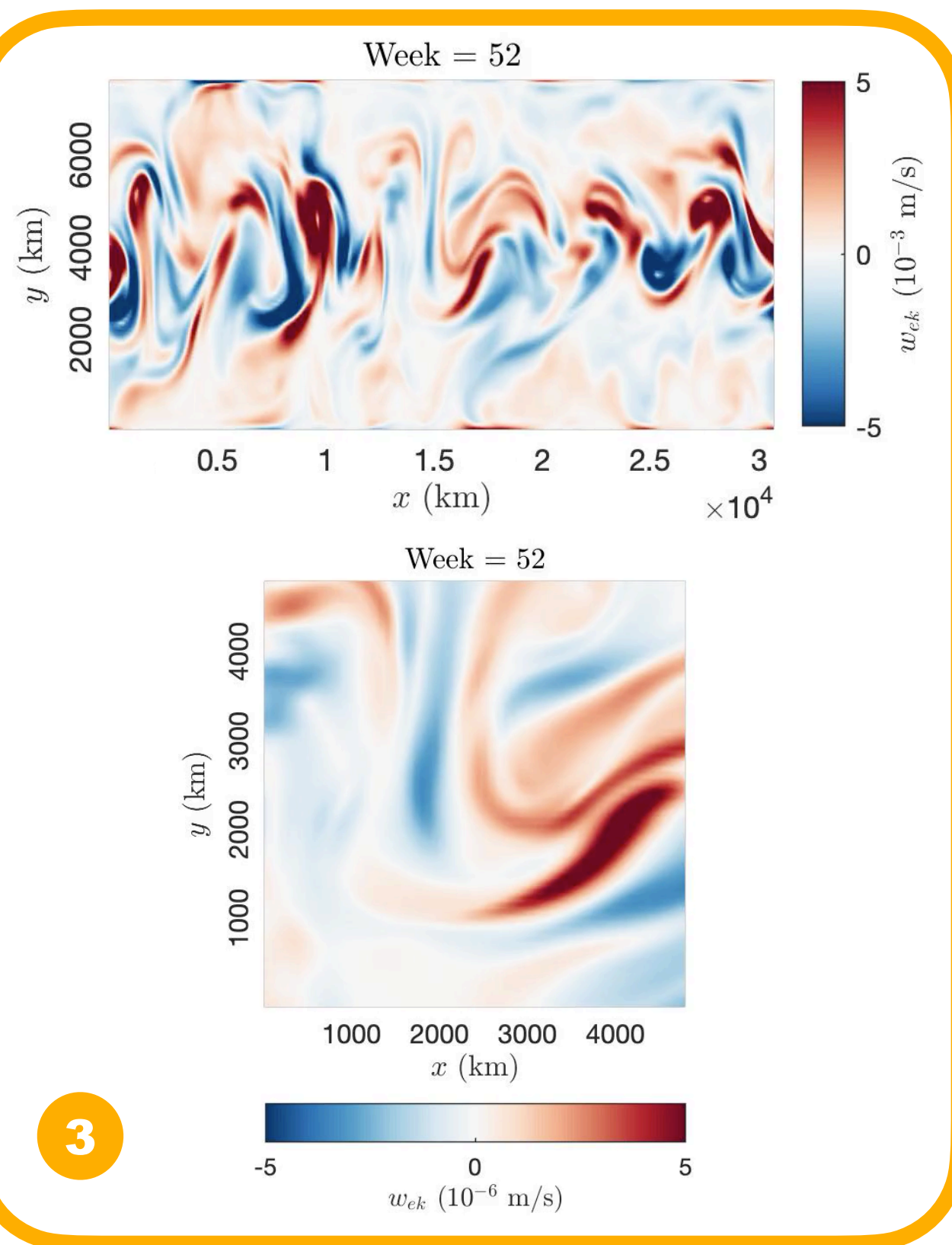
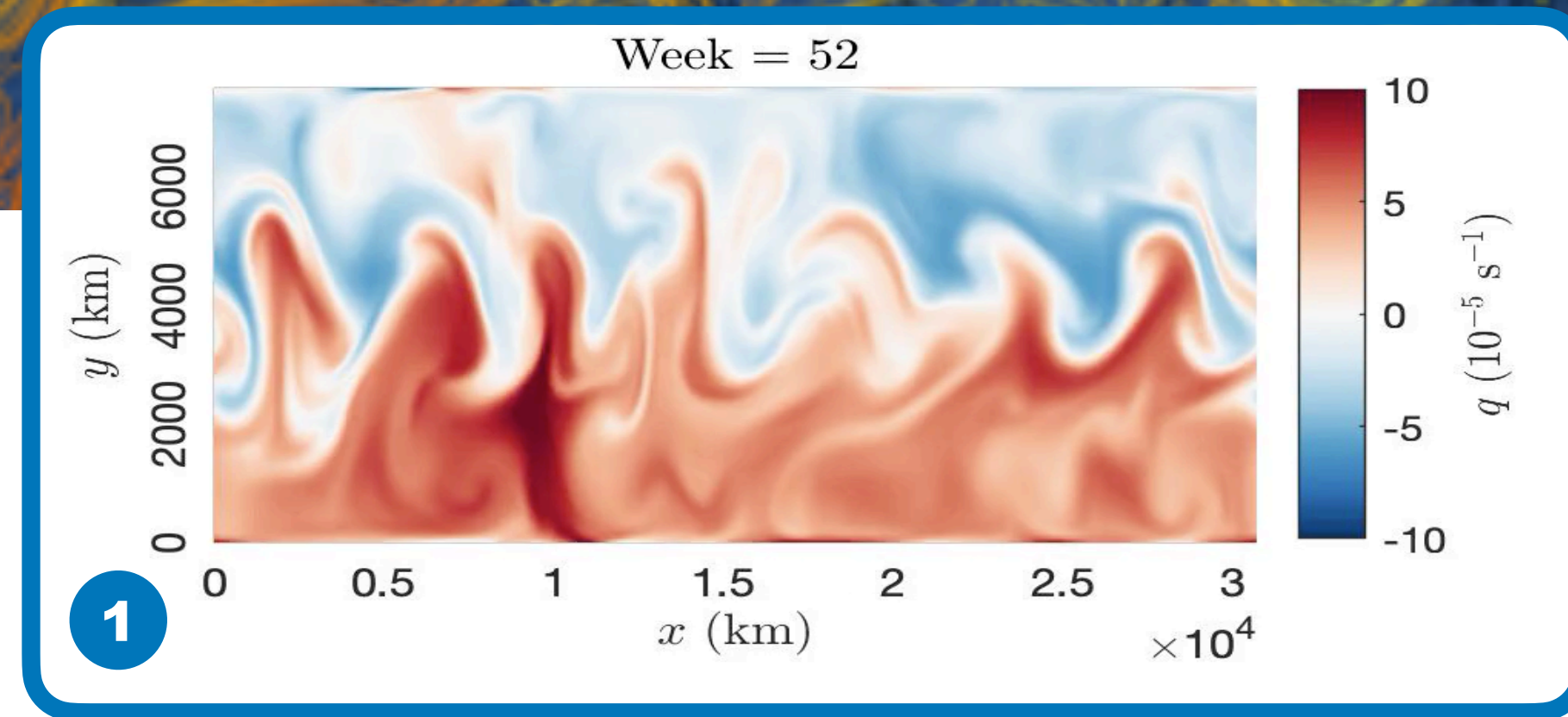


Comparison of contributions to the rate of KE for different coarse models (Exp.2)

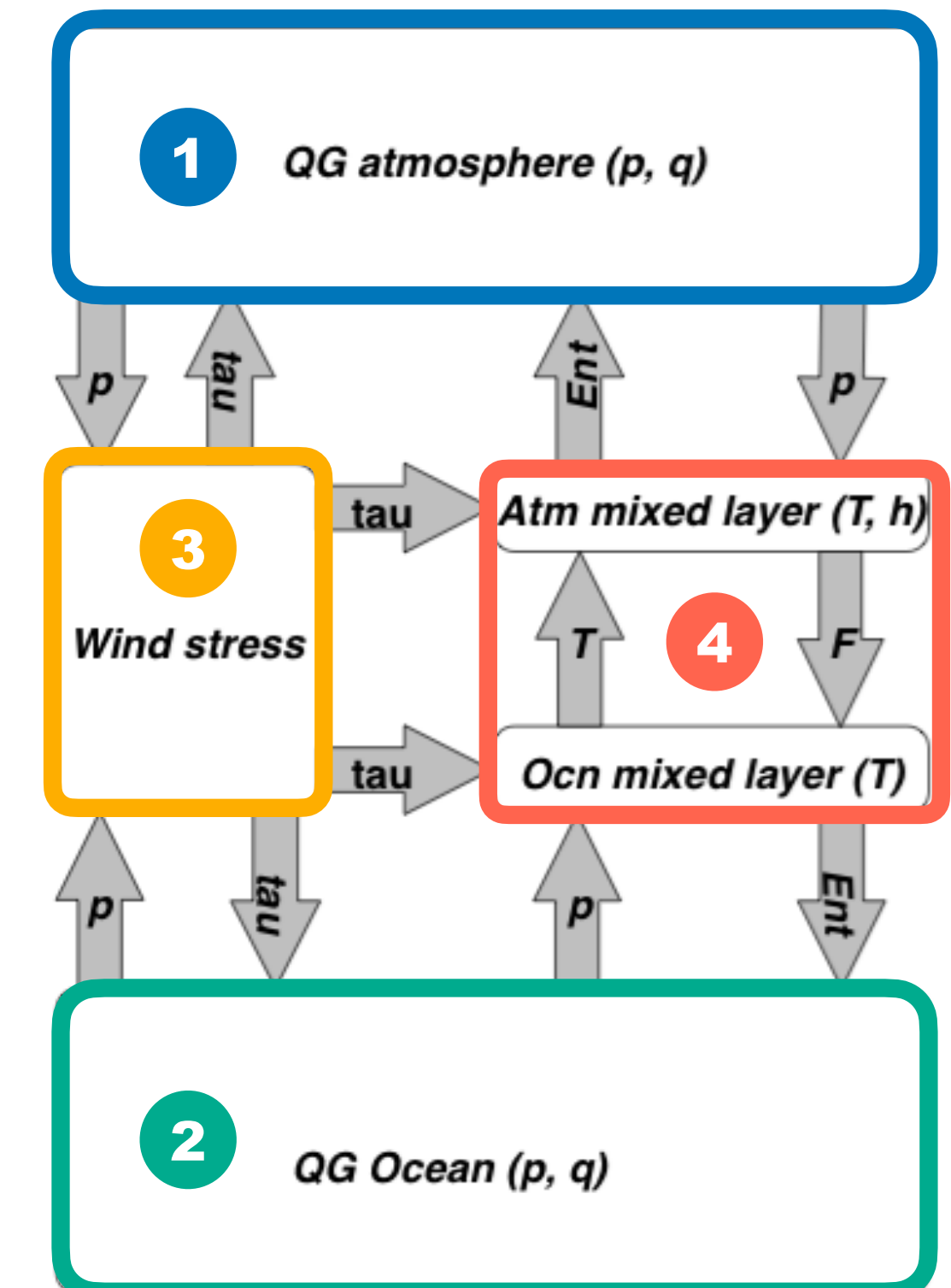
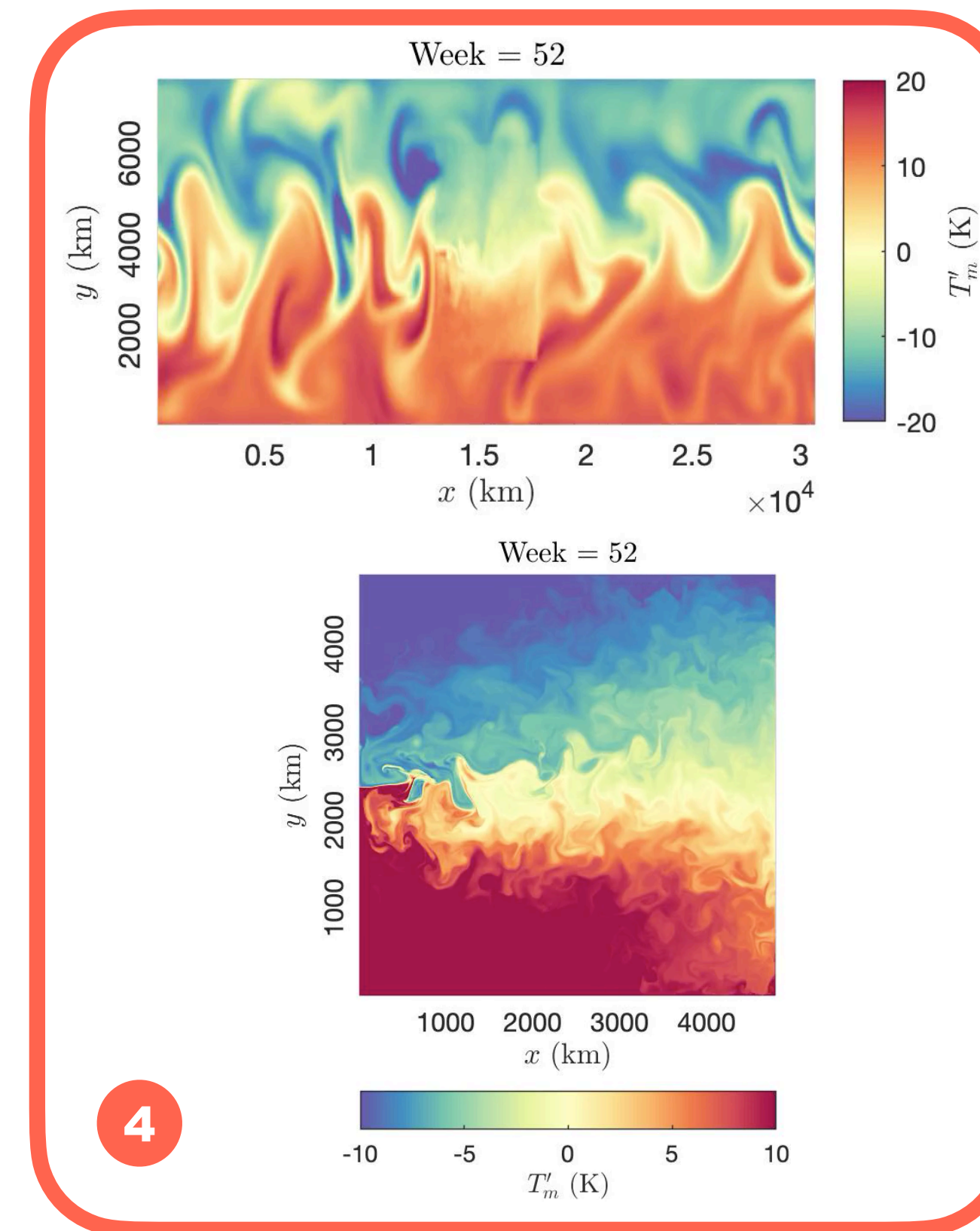
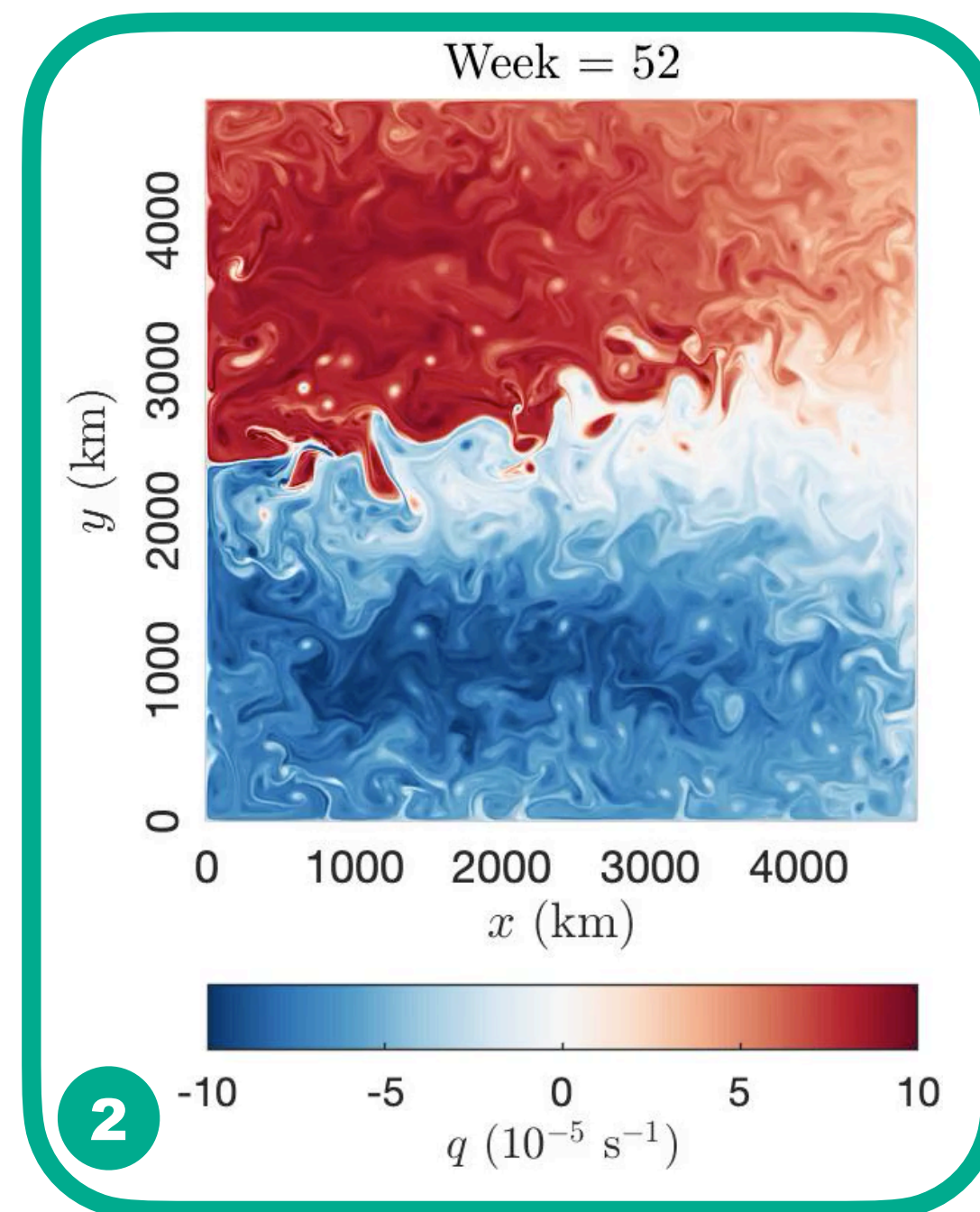
Conclusion

- The correction drift is found to be important in reproducing the meandering jet on coarse mesh.
- The non-stationary noise based on the projection method enables us to improve the low-frequency variability of the large-scale circulation.

Working on ...



Coupled model





Thanks for your attention !